SYNTHESIS AND CHARACTERIZATION OF THERMALLY STABLE DIELECTRIC FLUID FROM *AZADIRACHTA INDICA* SEED OIL

BY

SADIQ UMAR

DEPARTMENT OF PHYSICS

AHMADU BELLO UNIVERSITY, ZARIA

NIGERIA.

NOVRMBER, 2015.

SYNTHESIS AND CHARACTERIZATION OF THERMALLY STABLE DIELECTRIC FLUID FROM *AZADIRACHTA INDICA*SEED OIL

BY

Sadiq UMAR, BSc (ABU) 2011

MSc/SCI/41762/12-13

A DISSERTATION SUBMITTED TO THE SCHOOL OF POSTGRADUATE STUDIES,

AHMADU BELLO UNIVERSITY, ZARIA

IN PARTIAL FULFILLMENT OF THE REQUIREMENTS FOR THE AWARD

OF

MASTER DEGREE IN PHYSICS

DEPARTMENT OF PHYSICS,

FACULTY OF SCIENCE

AHMADU BELLO UNIVERSITY, ZARIA

NIGERIA

NOVEMBER, 2015.

DECLARATION

I declare that the work in this research dissertation entitled “Synthesis and Characterization of Thermally Stable Dielectric Fluid from *Azadirachta Indica*Seed Oil” has been carried out by me in the department of Physics. The information derived from the literature has been duly acknowledged in the text and a list of references provided. No part of this research thesis was previously presented for another degree or diploma at this or any other Institution.

Sadiq Umar		/11/2015
Name of Student	Signature	Date

CERTIFICATION

This project thesis entitled "SYNTHESIS AND CHARACTERIZATION OF THERMALLY STABLE DIELECTRIC FLUID FROM *AZADIRACHTA INDICA*SEED OIL" by SADIQ UMAR meets the regulations governing the award of the degree of MSc Physics of the Ahmadu Bello University, and is approved for its contribution to knowledge and literary presentation.

(Name) (Signature)

Dr A.A. Abdelmalik Date _____

Chairman, Supervisory Committee

(Name) (Signature)

Dr Sadiq Umar Date _____

Member, Supervisory Committee

(Name) (Signature)

Dr Sadiq Umar Date _____

Head of Department

(Name) (Signature)

Prof.KabiruBala Date _____

Dean, School of Postgraduate Studies

ACKNOWLEDGMENT

I wish to express my sincere appreciation to my supervisors; Dr AbdelghaffarAmoka Abdelmalik and Dr Sadiq Umar for giving me the opportunity to work under their supervision and guidance. I couldn't have done this without their guidance, encouragement, support and valuable suggestions. They have greatly influenced my academic and personal life.

Thanks to Muhammad Dabai, AlhajiLateef Suleiman, Ibrahim Sani, NuraLawal whom are all staffs of Physics Department ABU Zaria for their technical support during my Lab work, especially Muhammad Dabai for working with me both in his official and unofficial hours.

Also, I am grateful to my parents for their financial and moral support toward the success of this work, and to my friends and colleagues, I appreciate their support and encouragement.

Special thanks to The World Academy of Science (TWAS) for supporting this research work.

Finally, I wish to express my gratitude to Allah (SWA) for his infinite mercy and grace.

ABSTRACT

Epoxy neem and epoxy methyl ester samples have been synthesized and unsaturation which is responsible for thermo-oxidative instability of the oil eliminated through epoxidation reaction. Viscosity study of the samples over temperature range of 30°C to 90°C within intervals of 10°C shows Arrhenius type behaviour. The viscosity of the samples decreased exponentially with increase in temperature. Particle mobility in the samples is a thermally activated process with calculated activation energies of 0.21eV, 0.041eV and 0.038eV for the PNO, ENO and ENOE samples respectively.Dielectric response of the samples within frequency range of 20 Hz to 200 kHz at a temperature of 20°C show frequency independent permittivity which is indicative of a constant dominating charge transport mechanism.

Study of loss and electric conduction characteristics of the samples over frequency range of 20 to 200 kHz in the temperature range of 20 to 70°C was also carried out to understand the behaviour of the synthesized oils under electric field.Energy dissipationin the samples decreased with increasing frequency with slope of about -1. Dipolar polarization and ionic conduction dominates losses in the oils at high frequencies. Ions which resulted from the dissociation of molecules and from impurities introduced during processing, dominated electrical conduction in the samples. The measured ac conductivity of the samples is of the order of 10^{-10} Sm^{-1} to 10^{-7} Sm^{-1} and loss tangent is less than one (1.0) in the frequency range considered. The loss tangent and ac conductivity of the samples increased with increase in temperature. Charge transport in the oil samples is a thermally activated process with calculated activation energies of 0.34 eV, 0.37 eV and 0.32 eV for the PNO, ENO and ENOE respectively.

Comsol Multiphysics software was used to study field distributions in the fluid on application of high voltages in the range of 1 kV to 10 kV. A comparism of the maximum field produced in natural esters and transformer oils indicates that electric discharge is less favourable in natural ester fluid than in transformer oil. The presence ofair and water (impurities) in the oils led to reduced breakdown strength of the oils and could be source for initiation of surface discharge and consequently breakdown. It is suggested that the

synthesized fluid is similar to other synthesized natural ester fluid for use in electrical systems and as such could be a viable alternative insulation fluid for use in electrical systems.

TABLE OF CONTENTS

LIST OF TABLES

LIST OF FIGURES

LIST OF PLATES

ABBREVIATIONS

NARICT	-	National Research Institute of Chemical Technology
FTIR	-	Fourier Transform Infra-Red
PNO	-	Purified Neem Oil
ENOE	-	Epoxidized Neem Oil Ester
ENO	-	Epoxidized Neem Oil
PCB	-	Polychlorinated Biphenyl
POEs	-	Polyol Esters
PVC	-	Poly Vinyl Chloride
AIER	-	Acid Ion Exchange Resin
HV	-	High Voltage
AC	-	Alternating Current
DC	-	Direct Current
EDL	-	Electric Double Layer
SI	-	System Interntionale
CGS	-	Centimetre Gram Seconds (Gaussian Units)
ASTM	-	American Society for Testing and Materials
S/m	-	Siemen per Meter
ev	-	electron Volt
Pa.s	-	Pascal Seconds

CHAPTER ONE

INTRODUCTION

1.1 Research Background

Mineral oil has been used for several decades as insulating fluid in high-voltage equipment. However, issues associated with the production and use of the oil such as spills has raised environmental concern. Mineral oil is only poorly biodegradable and thus its long-term environmental pollution which consequently discourage its continual use in high voltage equipment. Also, mineral oil is in principle a limited resource that will eventually run out (Oommen, 2002). Hence, the need for an alternative industrial bio-based dielectric fluid from renewable sources that is biodegradable for ecological sustainability.

Vegetable oil has been identified as potential candidate for the synthesis of an effective bio-based dielectric fluid (Willing, 2001). Vegetable oil is readily available and comparatively inexpensive. They are triglycerides which are also known by the name triacylglyceride or TAG (see figure 1.1). In vegetable oil, glycerol molecule is attached to three fatty acid chains of unsaturated and saturated fatty acids. Many naturally occurring fats are composed of fatty acids with variation in chain length between 14-22 carbon atoms and single to triple bonds between neighbouring carbon atoms. The unsaturated fatty acids present in vegetable oil are oleic acid, linoleic acid and linoleic acid containing one, two and three double bonds between carbon-carbon atoms respectively. The functionality present in vegetable oil is in terms of double bonds and thus acts as a reaction site for chemical modification in vegetable oil (Saurabh*et al.*, 2011).

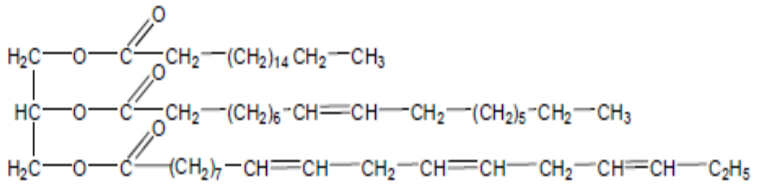

Figure 1.1: A triglyceride molecule

The carbon atoms in a double bond have three equivalent sp^2 hybrid orbits which lie in a plane at angles of 120° to one another (see figure 1.2). The fourth carbon orbital is an unhybridized p orbital perpendicular to the sp^2 plane. When two sp^2-hybridized carbon atoms approach each other a σ bond is formed through head-on overlap of the sp^2 orbitals and a π bond through sideways overlap of p orbitals and the doubly bonded carbons and the four attached atoms lie in a plane with bond angle of approximately 120° (McMurry, 2011).

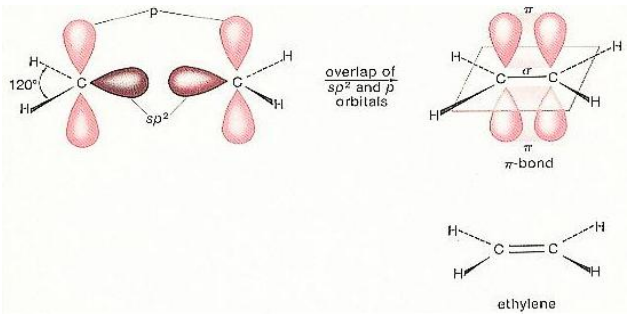

Figure 1.2: Ethylene orbital (meritnation.com)

Mono-unsaturated fatty acid has been shown to be more stable to oxidation than poly-unsaturated fatty acids. The ratio of relative instability due to unsaturation of fatty acids to oxidation is roughly estimated to be 1:10:100 for saturated, mono-, and poly-unsaturated C-18 triglycerides respectively (Oommen, 2002). The melting point of the oil decreases with the percentage of unsaturation. The unsaturated fatty acids generally have lower

melting points than the saturated fatty acids. The high pour point of saturated fatty acid results from its uniform molecular shape which enables the molecules to pack efficiently in a crystal lattice. On the other hand, crystal formation is difficult in unsaturated fatty acids because of the bends and kinks introduced by the carbon-carbon double bonds. This limits the ability of the fatty acids to be closely packed (McMurry, 2011).

Nevertheless, utilizing vegetable oil in the synthesis of dielectric fluid posits a major problem. Vegetable oils are esters of fatty acids and glycerol and are generally classified into two; one with high saturated fatty acids composition and hence more stable to oxidation but consequent high melting point, and the other with relatively high concentration of unsaturated fatty acids which is highly unstable to oxidation but possesses a low melting point (McMurry, 2011). Also, the thermo-oxidative stability is a function of the degree of saturation. Vegetable oil becomes more susceptible to oxidation as the degree of unsaturation progresses from mono-unsaturated to poly-unsaturated (Oommen, 2002). The challenge however is to develop a dielectric fluid with both low pour point and high thermo-oxidative stability, properties which are not inherently present all together in a class of the oil.

Chemical modification of the vegetable oil structure through the carbon-carbon double bond (unsaturation) could lead to an improved physco-chemical and electrical properties of the fluid (Erhan and Asadauskas, 2000). Epoxidation reaction of vegetable oil with high percentage unsaturation introduces epoxy groups into fatty acid unsaturated chains (i.e. the double-double bond functionality in the fatty acid chain) which have the effect of improving the physco-chemical and electrical properties of the fluid and widening its applicability (Knothe, 2007).

Characterization of the synthesized fluid over wide spectrum of frequency and temperature could reveal useful information on dielectric and electrical behaviour of the fluid.

Investigating some electrical properties of the developed fluid in a computer simulation not only allows for the evaluation and prediction of entities that may not be directly measurable in experiments but also allows for the exploration of the likely stressed regions in a prototype system where degradations that could lead to eventual failure is initiated.

1.2 Motivation

In Nigeria, Neem seed among several other non-edible seeds is available in abundance. Neem seeds especially are constantly seen on the floor of shelter belt areas constituting environmental nuisance. Knowing fully well how important the seeds can be processed into oil which could provide an alternative effective, affordable, renewable and environmentally friendly industrial fluid that could substitute the non-biodegradable and limited resource petroleum based products, motivated this research work.

1.3 Research questions

Non-edible seed based oil such as *Neem, Jatropha* and *Castor, etc.* composed of triglyceride ester which is made up of high concentration of unsaturated matrix of fatty acids (Atabani, 2013). Thermo-oxidative stability is a function of the degree of saturation. Vegetable oil becomes more susceptible to oxidation as the degree of unsaturation progresses from mono-unsaturation to poly-unsaturation although melting point of vegetable oil decreases with percentage unsaturation (Oommen, 2002). The question however is;

1. Can the oil be chemically modified to suit our purpose?
2. Can a suitable dielectric fluid that would be thermally stable to oxidation be developed from non-edible indigenous seed-based oil?
3. Can the oil be used for insulation in electrical systems?
4. Will the oil have competitive advantages with other dielectric fluids?

1.4 AIM

The aim of the research is to develop a thermally stable dielectric fluid from neem oil (i.e. non-edible seed oil) which possesses excellent dielectric and electrical properties that will make it suitable for use in various industrial applications.

1.5 OBJECTIVES

The research was designed to achieve the following;

- Extract and purify neem oil from neem seed
- Synthesize epoxy neem oil through an epoxidation reaction
- Synthesize alky ester of the epoxy neem oil samples (trans-esterification reaction).
- Performing structural and physical characterization of the synthesized fluid to determine how chemical modification affects the rheology of the fluid.
- Investigate dielectric response of the synthesized fluid over wide spectrum of frequency and temperature
- Relating measured characteristics to the chemical properties of the fluid
- Study field distribution in the developed fluid at high voltages in a computer simulation
- Suggest areas of applicability of the fluid

1.6 Justification

Mineral oil is a limited resource that will ultimately be exhausted. Non-edible seed-based oil on the other hand is technically and environmentally acceptable and is renewable resource that is available in abundance. For non-edible vegetable seed-based oil to qualify as industrial based fluid that could be used as dielectric, it must possess high and low temperature stability and excellent dielectric and electrical properties (Salih *et al.,* 2013). However these properties are inherent weaknesses in these oils which is as a result of high percentage unsaturated fatty acids composition. Chemical modification and some optimal extent of chemical alteration are necessary in other to eliminate completely poly-unsaturation to yield fluids with better thermal stability and improved physco-chemical and electrical properties.

1.7 Previous work done

Researches into the use of vegetable oil as bio-based stock for environmentally friendly, affordable and effective dielectric fluid have had several inputs. Challenges usually encountered by researchers in using a natural ester as dielectric fluid is developing an ester dielectric fluid with favourable low temperature properties (e.g. low pour point) and high oxidative stability. Nevertheless, vegetable oil possess among several other good properties, excellent biodegradability, low toxicity and low cost (Garces*et al.,* 2011). A published paper reported that purified and demoisturised coconut oil can be used satisfactorily as dielectric fluid in sealed distribution transformers in tropical climates (Lucas *et al*., 2001). But at about 23°C the oil freezes (this implies high pour point), although the breakdown strength of the coconut oil appeared to be independent of the state

of solidification the voids in the oil make it susceptible to partial discharges which could lead to degradation of the insulation. Also, due to the fact that the developed natural ester fluid is prone to oxidation, this consequently limits the use of the synthesized natural ester to hermetically sealed environment (Lucas *et al.*, 2001).

Nevertheless, in order to develop natural ester fluids that will not be restricted to use in hermetically sealed environment, poly-unsaturation will need to be eliminated to make the fluid less susceptible to oxidation. This can be achieved through chemical structural modification through processes of; hydrogenation, epoxidation, trans-esterification, etc., of fatty acids (Scrimgeour, 2005). Modification of chemical structure is becoming more popular as the modified oil may be used as raw material for environmentally friendly products. The introduction of epoxy groups into fatty acid unsaturated chains (epoxidation reaction) has been practiced for some time, following the pioneering work of Crivello's Laboratory; Epoxidation has received special attention because it opens up a wide range of feasible reactions that can be carried out under moderate reaction conditions due to the high reactivity of the oxirane ring (Salimon*et al.*, 2011). Epoxidized vegetable oils are of significant commercial interest. A common application is the use of epoxidized vegetable oil as plasticizer-stabilizer additive for poly vinyl chloride (PVC). Other uses include lubricating oils, composites, paint diluents, etc. (Knothe, 2007).

Epoxidation of soybean oil was reported to show 6.1 percent epoxy yield, the reason for the observed low yield may be due to presence of side reactions such as ring opening (Saremi*et al.*, 2012). Several researches have been carried out to optimize yield of

epoxidation of vegetable oil. Reports have shown that full epoxidation can be achieved using Acidic Ion Exchange Resin (AIER) as catalyst (Knothe, 2007).

There was also an attempt to produce insulating fluids through chemical modification of palm kernel oil. They achieved this by converting the oil into epoxy methyl ester. This was followed by opening the epoxy ring and drafting side chain on the ester structure to produce dielectric fluid. Result from the research show that the synthesized fluid possessed good thermo-oxidation stability and good low temperature properties (Abdelmalik *et al.*, 2010). Also, an increase in chain length led to a fluid with improved pour point. The synthesized fluid show excellent properties for use as industrial based fluid for various applications (Abdelmalik *et al.*,2011).

However, due to competing nature of the edible oils in use for electrical insulating purposes and their use for cooking purposes, in this research, Neem oil which is a non-edible source of vegetable oil was considered in producing a bio-base fluid for electrical insulation purposes.

In the current study the permittivity, loss tangent and AC conductivity were measured in the frequency range of 20 Hz to 200 kHz and temperature range of 20°C to 70°C, this allow for the study of dielectric properties of the developed fluid at low frequencies and at power frequency (50 Hz). The temperature dependency of dynamic viscosity of the fluid was also investigated over temperature range of 20°C to 90°C, at interval of 10°C to study how viscosity may affect conductivity of the fluid.

CHAPTER TWO

LITERATURE REVIEW

2.1 Background Theory

The science of dielectrics,which has been pursued for over a century is one of the oldest branches of physics and has close links to chemistry, materials science, and electrical engineering. The term dielectric was first coined by Faraday to suggest that there is something analogous to current flow through a capacitor during the charging process when current introduced at one electrode flows through the insulator to charge another electrode. The consequent of imposing a static external electric field across the capacitor, leads to the positively (ion core) and negatively (electron) charged species in the dielectric or insulator to become polarized. Charging occurs only as the field within the insulator is changing (William *et al.,* 2006). The physics of dielectrics involves the study of properties of dielectrics and the dependence of such properties on its structure and composition and also on various external factors such as impressed field and temperature. The fundamental properties/parameters which characterize a dielectric are its conductivity and real permittivity or dielectric constant.

The complex nature and structure of liquids has inhibited the development of a comprehensive liquid state theory. Rather, scientists have derived models and a basic understanding of processes in liquids by utilizing theories from both the solid-state and compressed gas-state.

Dielectrics are materials in which nearly all or a large portion of the energy required for its charging can be recovered when external electric field is removed

(Bartnikas, 2000). According to wave mechanical theory of the structure of matter, a dielectric is a material whose lower bands of allowed energy levels are completely full at absolute zero of temperature and at the same time isolated from higher unoccupied bands by a large zone of forbidden energy levels (Murphy and Morgan, 1938). Conduction in the lower fully occupied band is not favoured due to the fact that there are no unoccupied energy levels to take care of the additional energy which would be acquired by the electrons from the applied field, while the zone of forbidden energy levels is so wide (5 to 7 eV) that there is only a negligible probability that an electron in the lower band of allowed levels will acquire enough energy to make the transition to the unoccupied upper band where it could take part in conduction. Hence, a dielectric, subjected to an electric field, will evince only an extremely small conduction or loss current; this current will be caused by the finite number of free electrons available in addition to other free charge carriers (ions) associated usually with contamination by electrolytic impurities as well as dipole orientation losses arising with polar molecules under ac conditions. Often the two latter effects will tend to obscure the miniscule contribution of the relatively few free electrons available (Murphy and Morgan, 1938; Bartnikas, 2000).

Classically however, a material is dielectric due to the fact that electrons and other charged particles of which it is composed are held in equilibrium positions by constitutive forces characteristics of the structure of the material. When an electric field is applied however, these charges are displaced, but revert to their original equilibrium positions when the field is removed (Murphy and Morgan, 1938). Insulator materials are commonly called dielectric materials because all insulators have a dielectric constant. The dielectric constant determines the ability of the material to become electrically polarized and

determines it ability to hold an electrostatic field (Kaplan and McReynolds, 2002). Ideally, solid dielectrics are not conductors of electricity, so an applied field does not cause a flow of charge but instead causes relative displacement of opposite bound charges (on the scale of atomic diameter) and hence polarization of the material (Kasap*et al*., 2002).

In liquid dielectric materials, which are weak electrolyte, dissociation of ionic pairs generates free ions and ionic pairs are also formed by recombination of free ions. And, electric conduction in such fluid is as result of presence of ions in the fluid or injected charges from the electrodes. Hence application of electric field causes charge mobility and brings about recombination processes (Zadeh, 2011).

2.2 Dielectrics in Electrostatic field

In conductors, there are unlimited supplies of charges that are free to move about the material even with the slightest application of electric field. In practice it implies many of the electrons are not associated with any particular nucleus, but roam around at will. Contrary to this, dielectrics do not have free charges. All the charges remain attached to specific atom or molecule. The charges are known as bound charges and field produced by such systems of charges are called static fields, while the branch of electromagnetism studying such fields is called electrostatics. Nevertheless, these charges are able to be displaced forming dipoles within an atom or a molecule. The cumulative effects of such a displacement account for the characteristics behaviour of dielectric materials (Sharipov, 2003).

Classical electrostatics takes on its simplest form when it considers charges in vacuum. Such a system can be described by Poisson's equation given as:

$$-\nabla \cdot \nabla\varphi_e(\mathrm{r}) = \frac{\rho(r)}{\varepsilon_0} \qquad 2.1$$

and,$\boldsymbol{E}(r) = -\nabla\varphi_e(r)$. Where$\varphi_e(r)$ and $\rho(r)$are respectively the electrostatic potential and the charge density as a function of position r, and ε_0 is permittivity of vacuum. Intuitively, this equation implies that charges are the source of electrical field, since $-\nabla \cdot \nabla\varphi_e(r)$represents the divergence of the electric field $\boldsymbol{E}$. Also, the useful superposition principle can be deduced from Equation (2.1); which states; the total electrostatic field produced by a system of charges is the arithmetic sum of the fields produced by the individual charges. Hence, the field is the superposition of the individual fields (Gilson, 2006).

Electrostatic interactions among charges in a uniform medium (either gas, liquid, or solid) are usually weakened relative to those for the same charges in vacuum. Often to a good approximation, the field is reduced everywhere by a constant factor known as the dielectric constant also known as the relative permittivity ε_r. The permittivity expresses the ability of a dielectric material to polarize in response to an applied field. It is the ratio of the permittivity of the dielectric material to the permittivity of a vacuum,$(i.e.\ \varepsilon_r = \frac{\varepsilon}{\varepsilon_0})$.

For charges in a medium of uniform dielectric constant, the Poisson equation is written as:

$$-\nabla \cdot \nabla\varphi_e(\mathrm{r}) = \frac{\rho(r)}{\varepsilon} \qquad 2.2$$

This implies that the potentials that result from this equation are just $1/\varepsilon_r$for that in vacuum for the same charge distribution $\rho(r)$.

2.2.1 Induced Dipole

An atom or molecule in an externally impressed electrostatic field develops a nonzero net dipole moment. The magnitude of a dipole moment is a measure of charge separation.

The total dipole moment of a system of charges is given by the relation;

$$\mu = \sum_{all\ charges} q_i r_i \qquad 2.3$$

where r_i ,is the position vector of the charge q_i. The value of the sum will be independent of the origin chosen for the position vectors, provided that the system is neutral i.e. if the net dipole moment is zero.

The simplest case of an electric dipole is a positive and negative charge, so that the dipole is; $\mu = qd$ with q as the magnitude of each dipole charge and d the vector connecting the two charges. (Thus, an electron and proton separated by 1 Angstrom possess a dipole moment of 1 electron-Angstrom or in SI units, 1.65×10^{-29} Coulomb-meters.) Thus, the atoms or molecules in a material develop dipole moments when the material is exposed to an electrical field. The field generated by these induced dipoles runs against the inducing field. As a consequence, the overall field is weakened, as expected for a dielectric medium (Callister, 2001).

The total field produced by the dipoles is obtained from their potential. For a single dipole, the electrostatic potential can be found at any point distance r away from the dipole.

$$\varphi(r) = \frac{1}{4\pi\varepsilon_0}\frac{\hat{r}\cdot\vec{\mu}}{r^2} \qquad 2.4$$

And for dipole moments $\vec{\mu} = \vec{P}d\tau'$ in each volume element $d\tau'$, the total potential in the material is.

$$\varphi(r) = \frac{1}{4\pi\varepsilon_0}\int \frac{\hat{r}\cdot\vec{P}(r)}{r^2} d\tau' \qquad 2.5$$

And, the electric field produces by such a system of dipole is obtained from the relation (Zahn, 2003).

$$\vec{E}(r) = -\nabla\varphi(r) \qquad 2.6$$

2.2.2 Dielectric Polarization

Central to the physics of dielectrics is the polarization of the material, $\vec{P}$. Although atoms in dielectrics are electrically neutral, there is a positively charged core and a negatively charged electron cloud surrounding it. An impressed electrostatic field will cause the nucleus to push in the direction of the field and electrons in the opposite direction. In principle, if the field is large enough, it can pull the atom apart completely, ionizing it. However, with less extreme fields, equilibrium is soon established, for the positive core and negative electron attract one another and this holds the atoms together. The two opposing forces (i.e. *E* pulling the electron and nucleus apart, their mutual attraction drawing them together) reaches a balance, leaving the atom polarized, with plus charge shifted slightly one way and minus the other. The displacement of charged particles in atoms or molecules of dielectric material so that net dipole moment is developed in the material along the applied field direction is called polarization of the dielectric (Callister, 2001).

Considering a vacuum capacitor consisting of a pair of parallel electrodes having an area, *A*, and spaced, *d*, apart. If a potential difference, *V*, is applied between the electrodes, the field intensity at any point between the electrodes is$\vec{E} = V/d$. The capacitance of the vacuum capacitor is $C_0 = \varepsilon_0 A/d$ and the charge stored in the capacitor is

$$Q_0 = A\varepsilon_0\vec{E} \qquad 2.7$$

whereε_0 is permittivity of free space.

If a homogeneous dielectric material is introduced between the plates and keeping the potential constant, charge stored is given by

$$Q = \varepsilon_0 \varepsilon A\vec{E} \qquad 2.8$$

whereε is dielectric constant of the material. Since ε is always greater than one, $Q > Q_0$ and there is an increase in the stored charge given by;

$$Q - Q_0 = A\vec{E}\varepsilon_0(\varepsilon - 1) \qquad 2.9$$

this increase may be attributed to the appearance of charges on the dielectric surfaces.

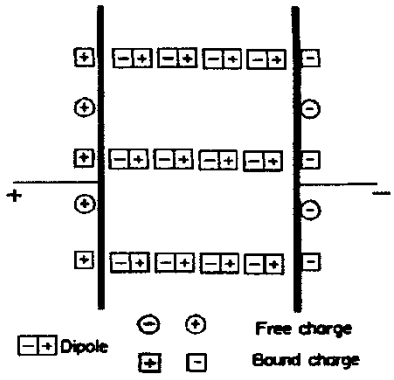

Figure 2.1: Schematic representation of dielectric polarization (Raju, 2003)

Figure 2.1 show effect of polarization in a dielectric, negative charges appear on the surface of the dielectric opposite to the positive plate and vice-versa. This system of charges is apparently neutral and possesses a dipole moment express as:

$$\vec{\mu} = A\vec{E}\varepsilon_0(\varepsilon - 1)d \qquad 2.10$$

since the volume of the dielectric is $v = Ad$ the dipole moment per unit volume is

$$\vec{P} = \frac{\vec{\mu}}{Ad} = \vec{E}\varepsilon_0(\varepsilon - 1) = \chi\varepsilon_0\vec{E} \qquad 2.11$$

the quantity P, is the polarization of the dielectric and denotes the dipole moment per unit volume Cm^{-2}. The constant $\chi = \varepsilon - 1$, is called the susceptibility of the dielectric medium.

The flux density D, is define as

$$\vec{D} = \varepsilon_0 \varepsilon \vec{E} \qquad 2.12$$

using this in equation 2.11, yields;

$$\vec{D} = \varepsilon_0 \vec{E} + \vec{P} \qquad 2.13$$

(Raju, 2003).

2.2.3 Electric Polarization Mechanisms

The dielectric behavior of materials is determined by the nature of the polarizations which an applied field induces in them. There are four mechanisms through which polarization takes place in dielectric materials;

i. Electronic or Optical polarization
ii. Ionic or Atomic polarization
iii. Orientational polarization
iv. Interfacial or space-charge polarization

2.2.3.1 Electronic polarization

This occurs when electrons are displaced relative to the nucleus. This polarization type is found in all dielectric materials, and exists only while static electric field is present. Polarization per unit volume due to electronic polarization can be considered to be a quantity which is proportional to the number of bound electrons in a unit volume and inversely proportional to the forces binding them to the nuclei of the atom. For instance,

the dielectric constant of liquid nitrogen is 1.43, which is much higher than the value 1.000600 for the gas. This is due to the fact that the number of molecules, and consequently of bound charges per unit volume is much greater in the liquid than in the gas. The polarization is define as

$$\vec{P} = \vec{E}\varepsilon_0(\varepsilon - 1) = N\alpha_e\vec{E} \qquad 2.14$$

the dipole moment induced in an electronically polarized atom is proportional to the internal field $\vec{E}_{loc}$ which is the increase in the electric field experienced by a molecule due to the polarization of the surrounding molecules.

$$\vec{\mu}_e = \alpha_e\vec{E}_{loc} \qquad 2.15$$

whereα_e is the electronic polarizability. Polarizability refers to the proportionality constant for the formation of dipole under the influence of electric field. Thus its value is typical for each different type of atom or molecule (Raju, 2003). Physically, polarizability is induced when there is electric field applied onto the materials. In the absence of electric field, the electrons are distributed evenly around the nuclei. When the electric field is applied the electron cloud is displaced from the nuclei in the direction opposite to the applied field. This result in separation of positive and negative charges and the molecules behave like an electric dipole (Ahmad, 2012).

2.2.3.2 Ionic polarization

This occurs when cations and anions are displaced relative to each other; an applied field acts to displace cations in one direction and anions in the opposite direction, which gives rise to a net dipole moment. Ionic polarization occurs in all molecules but it is more pronounced in molecules that have relatively weak bonds.

The charge displacement in the presence of dc fields involves changes in bond length and bond angle, in addition to bending or twisting of polar groups with respect to each other. The displacement is restricted by the degree of vibrational freedom of the molecule.

The polarization can be obtained from the expression (Raju, 2003).

$$\vec{P} = N\vec{E}_{loc}(\alpha_e + \alpha_a + \frac{\mu^2}{3K_BT}) \quad 2.16$$

2.2.3.3 Orientation polarization

This occurs when permanent dipoles, such as water (H_2O) molecules are aligned; Debye postulated that the molecules of all substances except those in which the charges are symmetrically located possess a permanent electric moment which is characteristic of the molecule. In liquid or gas these molecular dipoles are oriented at random and therefore the magnitude of the polarization vector is zero. However, when static electric field is applied, there is a tendency for the molecules to align themselves with their dipole axes in the direction of the applied field.

However, in real dielectrics, the tendency of dipoles to orient in the direction of an applied field will be counteracted by random collisions between molecules, a process driven by thermal energy 'KT' at a temperature 'T'. Therefore, basically when an external field is impressed, there is a competition between the field induced order and thermal driven disorder. The later (i.e. thermal driven disorder) prevails in liquids more than in solids. Hence, perfect alignment of dipoles would only be possible at low temperatures and possibly in solid crystals.

The dipole moment, often called Langevin-Debye equation is given as

$$\vec{\mu}_o = \frac{\mu^2\vec{E}}{3K_BT} = \alpha_d\vec{E} \quad 2.17$$

where,μ_o, is the average contribution of the molecules to the polarization of the material, and μ, is the inherent dipole moment due to the structure of the molecules of the material. And the polarization of the material is

$$\vec{P} = N\alpha_o\vec{E} = \frac{N\mu^2\vec{E}}{3K_BT} \qquad 2.18$$

this equation is referred to as the Debye equation. When fields are high and temperature is very low (i.e. minimizing the randomization), all the dipoles would be parallel to the applied field and then the average dipole moment would be equal to the theoretical dipole moment (Raju, 2003). Electronic polarization is unaffected by temperature (i.e. it is instantaneous), However, atomic and ionic vibrations are affected by temperature. The binding force between ions or atoms is weakened by increased temperature.

2.2.3.4 Interfacial polarization

Also known as space charge polarization, unlike the electronic, atomic, and orientation polarization which occurs when charges are locally bound in atoms, molecules, or structures of solids or liquids, charge carriers also exist that can migrate over a distance through the material when a low frequency electric field is applied. Interfacial or space charge polarization occurs when the motion of these migrating charges is impeded. The charges can become trapped within the interfaces of a material. Motion may also be impeded when charges cannot be freely discharged or replaced at the electrodes. The field distortion caused by the accumulation of these charges increases the overall capacitance of a material which appears as an increase in dielectric constant.

The total polarization of a material is equal to the sum of the electronic, ionic, orientation and space charge polarizations (P_e, P_i, P_o, and P_s respectively). It is possible for one or more of these contributions to the total polarization to be either absent or negligible in

magnitude relative to the others. For example, ionic polarization will not exist in covalently bonded materials in which no ions are present (Murphy and Morgan, 1938; Callister, 2001).

2.3 Dielectric Dispersion

Dielectric dispersion is the dependence of the permittivity of a dielectric material on the frequency of an applied electric field. Dipole formation as explained is a result of electronic polarization (displacement of electrons), distortion polarization (displacement of ions), or orientation polarization (displacement of molecules) in an alternating electric field. These phenomena have characteristic dependence on the frequency of the alternating electric field, giving rise to a change in the real and imaginary part of the dielectric constant between the microwave, ultraviolet, and optical frequency range.

In many practical applications, dielectrics are used under time varying field. For a dielectric material that is subject to polarization by time varying electric field, with each direction reversal, the dipoles attempt to reorient with the field, a process requiring some finite time. For each polarization type, some minimum reorientation time exists which depends on the ease with which the particular dipoles are capable of realignment. A relaxation frequency f_m, is taken as the reciprocal of this minimum reorientation time τ (i.e relaxation time) and expressed as (Murphy and Morgan, 1938; Callister, 2001);

$$f_m = {}^{1}/_{2\pi\tau} \qquad 2.19$$

a dipole cannot keep shifting orientation direction when the frequency of the applied electric field exceeds its relaxation frequency, and therefore, will not make a contribution to the dielectric constant. The dependence of dielectric constant ε_r on the field frequency is represented schematically in Figure 2.2. The dielectric constant displays a maximum

before a symmetrical drop about a certain frequency. These maximum and minimum represent the optimum polarization in phase with the oscillating frequency. When a polarization mechanism ceases to function, there is an abrupt drop in the dielectric constant; otherwise, it is virtually frequency independent.

The mechanism for electronic polarization occurs at higher frequency (shorter wavelength e.g. infra-red region). This region involves excitation of electrons which is characterized by the quantized energy level hence is known as resonance behaviour. The frequency at which the turning point occurs is termed the natural frequency. At this point the frequency of applied electric field is at resonant with the natural frequency and hence there is a maximum absorption. Consequently this leads to maximum dielectric loss (Dielectric loss is the absorption of electrical energy by a dielectric material that is subjected to an alternating electric field). A low dielectric loss is desired at the frequency of utilization.

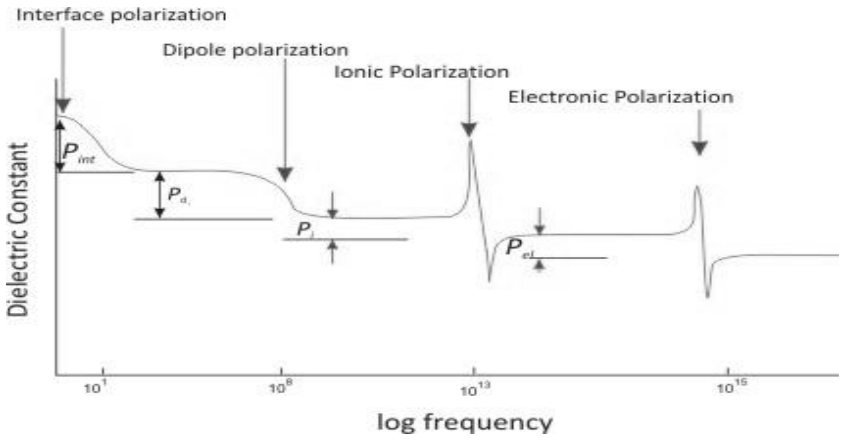

Figure 2.2: The variation of dielectric constant with frequency of an alternating electric field

Intuitively, it can be mentioned that the heavier the particular entity the more the time spent in displacing it (only the low mass bodies of the electrons can polarize in response to very high frequency electric fields). As a result, atomic polarization is the fastest and typically persists at frequencies between ~10^{13}-10^{15} Hz. In contrast, ionic polarization is

sluggish and typically occurs at frequencies between ~10^9-10^{13} Hz while dipolar polarization involving movement of molecules happens below 10^9 Hz. Interface or space charge polarization occurs at frequencies below 10^1 Hz (Callister, 2001).

Electrical insulating fluids are used to insulate the high and low voltage parts of oil-filled electrical equipment (transformers, switchgear, etc.). The behaviour of the dielectric fluid is associated with their molecular structure, operating temperature, and applied field. In Nigeria, electrical equipment operates at frequency of 50 Hz, characterization of dielectrics over wide range of frequency enable the understanding of the behaviour of the material since the response of the material varies with frequency variation. For instance, knowledge of the behaviour of charged particles in dielectrics and the molecular behaviour of the dielectrics can be obtained at low and higher frequencies. The response at low and high frequencies in the range of 20 Hz and 200 kHz can reveal useful information about the behavior of free charges and this can be used to identify the character of the conducting ions.

2.4 Charge Transport (Dielectric Conductivity)

An ideal dielectric material has finite dielectric loss and in simple terms can be said to behave like a parallel RC circuit. Hence, the behaviour of a dielectric material can be described by the means of an equivalent parallel RC circuit as shown in figure 2.3 With C representing the capacitance and R the large resistance of the dielectric. On application of an alternating field to a capacitor with two plane parallel electrodes in vacuum,

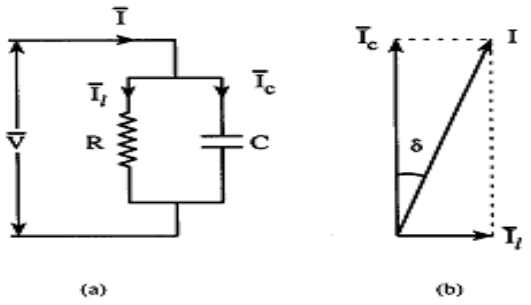

Figure 2.3: (a) parallel equivallent RC circuit (b) corresponding phasor diagram

If a parallel plate with a vacuum in between is considered, the stored charges on application of a sinusoidal field;

$$\bar{V} = \bar{V}_0 \exp(i\omega t) \qquad 2.20$$

where $\omega = 2\pi f$, is angular frequency and f is the driving frequency is given by;

$$Q = C_0 \bar{V} \qquad 2.21$$

where C_0 is vacuum capacitance of the capacitor, i.e. when vacuum is the dielectric between the two parallel plates. The charging current through such a capacitor is

$$\bar{I}_c = \frac{dQ}{dt} = C_0 \frac{d\bar{V}}{dt} = i\omega C_0 \bar{V} \qquad 2.22$$

and leads the voltage by a phase angle of 90˚.When the space between the parallel plates is filled with the dielectric material, the capacitance increases to

$$C = \frac{C_0 \varepsilon}{\varepsilon_0} = C_0 \varepsilon_r \qquad 2.23$$

where, ε_r, is the relative permittivity, ε, is the permittivity of the dielectric material and ε_0, is the permittivity of vacuum. The charging current becomes

$$\bar{I}_c = i\omega C \bar{V} \qquad 2.24$$

phasor diagram as shown in Figure 2.3(b) can be used to represent the complex permittivity of the dielectric material represented as RC in Figure 2.3(a) The charging current and loss current are 90˚ out of phase and cannot be added directly. The total current will depend upon the resistance, R and the reactance of the capacitor, X_C, and has phase difference with the applied voltage. The loss current in the dielectric material resulting from drifting of charges is characterized by dc conductivity of the material. This is often referred to as volume conductivity. The loss current component (I_l) is in phase with the voltage and is expressed in terms of G, the conductance of the dielectric as

$$\bar{I}_l = G\bar{V} \qquad 2.25$$

the total current can be expressed as

$$I = I_l + I_c = (G + i\omega C)\bar{V} \qquad 2.26$$

for a real dielectric, the current phasor will not be in phase with the voltage but by an angle (90˚-δ) where δ is refer to as the loss angle. The complex permittivity is defined as

$$\varepsilon^* = \varepsilon' - i\varepsilon'' \qquad 2.27$$

it consists of the real part which is the dielectric constant and the imaginary part which is the dielectric loss

In a dielectric material, the charging current is accompanied by a loss current associated with storage of electric charge by the dipoles. There are two sources of this loss current;

1. Long range migration of charges due to Ohmic conduction and it is frequency independent i.e. dc in nature
2. Dissipation of energy due to dipole rotation or oscillation as there is always certain inertia due to the movement of their mass. This contribution is time dependent i.e frequency dependent.

The total current through dielectric material can be completely defined using the geometry of the capacitor

$$\bar{I} = \frac{i\omega\varepsilon^* A\bar{V}}{d} = i\omega\varepsilon^* A\bar{E} \quad 2.28$$

and the total current density is

$$\bar{J} = \frac{\bar{I}}{A} = i\omega\varepsilon^*\bar{E} \quad 2.29$$

using equation in

$$\bar{J} = (i\omega\varepsilon' + \omega\varepsilon'')\bar{E} = \bar{J}_c + \bar{J}_l \quad 2.30$$

where, $\bar{J}_c \; and \; \bar{J}_l$are the capacitive and leakage current density of the total current density respectively.

The frequency response can be expressed in terms of the ratio of the leakage current to capacitive current. It is referred to as loss tangent, i.e.

$$\tan\delta = \frac{\bar{J}_l}{\bar{J}_c} = \frac{\varepsilon''}{\varepsilon'} = \frac{1}{\omega RC} = \frac{\sigma}{\omega\varepsilon'} \quad 2.31$$

whereσ is conductivity of the dielectric in S/cm, defined as the ratio of the leakage current density to the electric field;

$$\sigma = \frac{\bar{J}_l}{\bar{E}} = \omega\varepsilon'' \quad 2.32$$

and can also be expressed as

$$\sigma = \sum(q_i N_i \mu_i) \quad 2.33$$

where, q_i is the charge of ions of types i in Coulomb, N_i is the concentration of mobile ionic impurities in m^{-3}, and μ_i is the ionic mobility in $m^2 \cdot V^{-1} \cdot s^{-1}$, the charge mobility is dependent on viscosity, temperature and molecular collision. With the assumption that the impurity ions are spheres of radii r_0, using Stoke's law, the ionic mobility of the ionic impurities in dielectric liquid can be approximated as

$$\mu_{ion} = \frac{q}{C\pi\eta r_0} \quad 2.34$$

where, η is the dynamic viscosity. If a few layers of the liquid are tightly bound to the particle, sticking condition, the constant C=6 and if the contact is minimal, slipping condition, the constant C=4. The conductivity becomes

$$\sigma = \frac{q^2 N}{C\pi\eta r_0} \quad 2.35$$

as these impurities charges drift through the liquid, they may undergo electrode polarization and the charges accumulate at the interfaces between the bulk liquid and the electrodes. This results in the formation of a thin layer of charges with high capacitance at the electrode-liquid interface. This layer is known as electric double layer (EDL). The ac conductivity is given by

$$\sigma_{ac} = \sigma' + i\sigma'' = \omega\varepsilon_0[\varepsilon'' + i(\varepsilon' - \varepsilon_\infty)] \quad 2.36$$

the motion of charges in the dielectric gives rise to the conduction of current and additionally polarizes the dielectric. The conductivity may be visualized as contributing to the dielectric loss. This equation gives the contribution of conductivity to the dielectric loss. The total conductivity is given by;

$$\sigma_T = \sigma_{ac} + \sigma_{dc} = \omega\varepsilon_0\varepsilon'' + \sigma_{dc} \quad 2.37$$

(Raju, 2003).

2.5 Dielectric breakdown

Electrical breakdown occurs when the dielectric strength which is the maximum electric field applicable on dielectric material is exceeded. It underwent catastrophic failure leading to short circuit or blown fuse. This occurs when at a given applied voltage the heat generated due to the losses is greater than the heat dissipated and if the voltage is applied

for long enough periods then the dielectric is unable to reach a state of internal thermal equilibrium. The favourable condition for the occurrence of breakdown is large thickness of the dielectric, high temperature of both the dielectric and the surrounding, continuous application of high voltage and large dielectric loss (high tan δ). The last factor is the most important to occur at high frequency. The high humidity in air can similarly affect dielectric breakdown through electrolytic process (Ahmad, 2012).

Due to major implications of insulation failure such as damage to power equipment and surrounding environment also financial loss, researchers have been studying the insulating properties of dielectric fluids in other to understand the mechanisms (intrinsic, thermal, Avalanche, etc.) behind breakdown so as to reduce the likelihood of breakdown. Much focus has been centered on the formation of electrical streamers. Electrical streamers are low density conductive structures that form in regions of oil that are overstressed by electric fields on the order of $1 \times 10^8\ V/m$ or greater. Once formed, electrical streamer elongates, growing from the point of initiation towards a grounded point. The extent of which depend on the nature of the electrical excitation (magnitude, duration, rise time, etc) which caused it. Sustained over-excitation can result in a streamer short circuiting the oil gap between electrodes. In such a situation electric breakdown arc will form (Hwang*et al.*, 2010). A study of streamer propagation in rapeseed oil was carried out by Duy*et al.* (2007), they reported that the properties of streamers in natural ester fluids are less favourable for high voltage insulation than mineral oil.

2.6 Liquid Rheology

Rheology is simply the study of the deformation and flow of matter. And, viscosity is a measure of the resistance offered by such matter to a deforming

force. Also,an interesting property of insulating fluid is how its viscosity influence charge transport in the liquid. A liquid with high viscosity that appears to have low dielectric loss may become lossy with increase in temperature when impurities in the liquid become mobile. Models for predicting the viscosities of liquid are much less developed than those of gases and their use is limited to a qualitative description of observed behaviour. Unlike in gases, the viscosity of liquids decreases with increasing temperature. The relationship can be expressed in form of an Arrhenius-type equation;

$$\eta = Ae^{E_a/KT} \qquad 2.38$$

where η is viscosity (Pa.s), K is Boltzmann constant (8.6173324×10^{-5} eV/K), T is temperature in Kelvin (K), A is the pre-exponential term (Pa.s) and E_a is the activation energy (eV) which can be determine from the slope of a plot of ln(η) against 1/T. The mobility of the liquid molecule is a temperature-activated process.

In recent years, interest has been on developing industrial fluids from oil seed crops different from those used for food production. This will have the advantage of not directly competing with food stocks, which will involve rising the world market price of food. Non-edible vegetable seed-based oil such as Neem, Jatropha, Karanja, Castor, etc., are equally biodegradable and renewable as the edible vegetable seed-based oils and in addition have effectively comparable cost and availability (Jain and Suhane, 2012).

2.6.1 Neem (*Azadirachta indica*):Neem tree belongs to the *Meliaceae*family. It is a multipurpose and an evergreen tree, 12–18 m tall, which can grow in almost all kinds of soil including clay, saline, alkaline, dry, stony, shallow soils and even on solid having high calcareous soil. It is native to India, Pakistan, Sri Lanka, Burma, Malaya, Indonesia, Japan, and the tropical regions of Australia. It thrives well in arid and semi-arid climate with

maximum shade temperature as high as 49°C and the rainfall is as low as 250 mm. It can be raised by directly sowing its seed or by transplanting nursery-raised seedlings in monsoon rains. It reaches maximum productivity after15 years and has a life span of 150–200 years. A mature Neem tree produces 30–50 kg fruit. Neem kernel is found to possess an oil content of about 40-50% (Atabani*et al.*, 2013).

Table 2.1 Fatty acid profile of Neem seed oil in wt% (Atabani*et al.*, 2013; Top-Notch Technology…, 2014)

Fatty Acids	Common name	Structure	Percentage
C16:0	Palmic	$CH_3(CH_2)_{14}COOH$	14.9
C18:0	Stearic	$CH_3(CH_2)_{16}COOH$	20.6
C18:1 9c	Oleic	$CH_3(CH_2)_7CH{=}CH(CH_2)_7COOH$	43.9
C18:2 9c12c	Lioleic	$CH_3(CH_2)_3(CH_2CH{=}CH)_2(CH_2)_7COOH$	17.0
Others	-	-	3.7

Non-edible seed-based vegetable oils are composed mostly of high percentage unsaturated fatty acids as shown in table 2.1; this makes it unstable to oxidation and hence undesirable for use in developing dielectric fluid. However, as earlier stated, modification of chemical structure of vegetable oil with high percentage poly-unsaturation, could lead to synthesized fluid with desirable properties for effective use as dielectrics and in other industrial applications. In this research work, attempt has been made on chemical modification of a non-edible Nigerian seed-based oil (Neem oil) to improve its chemical stability and study the physco-chemical and electrical properties of the fluid for its possible consideration as high voltage insulation fluid.

CHAPTER THREE

MATERIALS METHOD

3.1 Materials

Major equipments used in synthesis and characterization of samples includes; Programmable LCR Bridge{A Rohde and Schwarz Company, H8118},Digital Viscometer {Brookfield,RVDV-I},thermostatically controlled rotary hot plate{IKA, C-MAG HS10}, Vacuum oven {Cheng Sang, Jin-Mao Science Technology Instrument Enterprise Co., Ltd}, Mini Oven {Scientific Equipment and Service, India}.

Also, solvents used includes; Citric acid {$C_6H_8O_7$, purity: 99.7%, AnalaR BDH chemical ltd, Poole, England}, Glacial acetic acidAnalaR {$C_2H_4O_2$, purity: 99.8%}, Toluene {$C_6H_5CH_3$, purity: 99.7% BDH Limited Poole, England}, MethanolAnalaR {CH_3OH, purity: 99.8%, BDH chemical ltd, Poole England}, Sodium hydroxide {MERCK Darmstadt, Germany}, Silica gel {incorporating 13% calcium sulphate, BDH chemical Ltd Poole, England}, Sodium sulphate anhydrous {BDH chemical Ltd, Poole England},Hydrogen Peroxide {about 30% H2O2 GPR, assay 30-31%, BDH chemical ltd}, 24cm Filter paper, medium crystalline {Whatman, England}.

3.2 Sample Purification

Crude sample of the oil was purchased from the National Research Institute for Chemical Technology (NARICT), Zaria and then purified as follows;

- 200 ml crude sample of neem oil was heated in a 500 ml conical flask to 70˚C and 8% volume of 64% aqueous citric acid solution was added gently and mixed thoroughly with a magnetic stirrer for 15 min.
- 4 ml of 8% NaOH solution was gently added and the mixture magnetically stirred at 400 rpm for 15 min. the mixture was then dried in vacuum oven at 85°C for 30 min to reduce the water content
- 2 g silica gel was added to the mixture at 70°C and agitated for 30 min at 300 rpm to prevent it from settling out
- Fuller's earth was then added and magnetically stirred for 30 min at 85%
- The sample was then filtered in vacuum oven at 85°C using a filter paper.

3.3 Synthesis of Epoxidized Neem Oil (ENO) and Epoxy Neem Oil Ester (ENOE)

Epoxidation is the reaction by which a double bond (unsaturation) is converted to an epoxide.Thereaction was carried out in a 1 litre three necked round bottom flask, equipped with a magnetic stirrer and placed in a water bath. The central neck of the flask was connected to a reflux condenser and a thermometer to one of the side necks in order to record the temperature of the reaction mixture,

- 50 g purified sample of the oil was poured into the flask, 12.5 g glacial acetic acid (CH_3-COOH) i.e. 0.5:1 acetic to ethylenic unsaturation molar ratio was added to the oil in the flask and 12.8 g toluene was then added to the mixture in the flask and the mixture moderately stirred and heated to a constant temperature of 55°C.
- 12.5 g of 2% H_2SO_4 was loaded into 35 g of 30% aqueous hydrogen peroxide (H_2O_2) (i.e. 1.5moles of H_2O_2 per 1mole of ethylenic unsaturation) in a 250 ml

quick-fit separatory funnel fit to one of the neck of the reactor flask and added in drops to the mixture in the reactor and the mixture stirred until the addition was completed. The reaction was allowed to continue for 4hours at moderate stirring speed at 55°C.

- On completion, the reaction mixture was placed in a separatory funnel and the bottom layer was discarded and the upper layer was collected and washed with cold distilled water 3times and then with slightly hot distilled water.
- The sample was then dried over sodium sulfate

Finally, the sample was placed in a vacuum oven at 80°C to get rid of excess toluene in the sample. Aliquot were collected in a sampling bottle for Fourier Transform Infra-Red (FTIR) Analysis in other to determine success of the reaction and hence oxirane content

Epoxy methy ester sample of the oil was produced by transesterification of the epoxidized neem oil sample (ENO). Transesterification (Alcoholysis)is the reaction of an alcohol and an ester to form different alcohols and esters. The process is called methanolysis when the alcohol used is methanol and ethanolysis when ethanol is used. The reaction was performed in a 250 ml flat bottom glass. 50 g of the ENO sample was introduced into the glass vessel along with a magnetic stir bar.

- 15 ml methanol was then added to the oil sample in the flask. Followed by the addition of 0.5 g (1% weight) NaOH into the mixture.
- The mixture was then heated to 50°C on a hotplate and magnetically stirred at rotation speed of 500 rpm. And the reaction was stopped after 2hrs and the reaction

mixture transferred to a 500 ml separatory funnel and left for some hours (about 4hrs) to separate. The bottom layer was discarded and the top layer collected.

- The collected mixture was washed with 0.015 M phosphoric acid 4times, the emulsion was kept in oven for one hour for separation. The bottom layer which contains remnant glycerol and NaOH was discarded and the top layer containing alkyl ester of the oil and methanol was collected and dried over anhydrous sodium sulfate.
- Finally the collected sample was then heated in vacuum oven at temperature slightly above boiling point of methanol for about 2-3hrs to remove excess methanol. Aliquot were taken for FTIR analysis. Plate I and table 3.1 show the various samples and their description respectively.

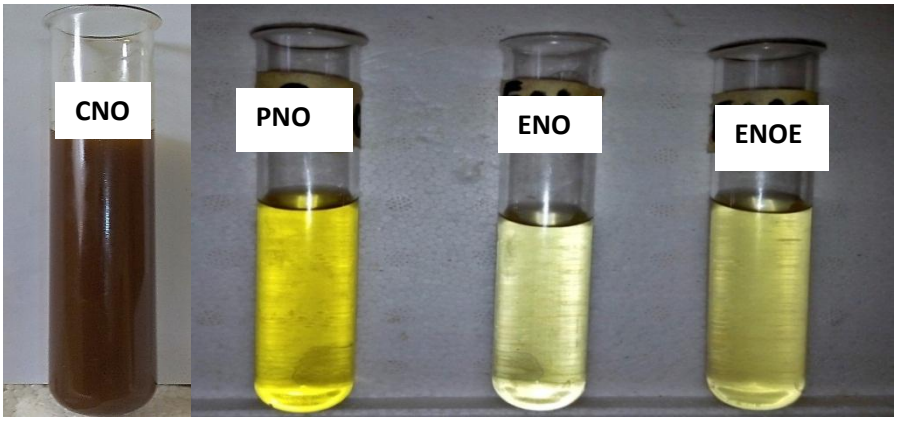

Plate I: Samples

Table 3.1: Sample description

Samples	Description
CNO	Crude Neem Oil
PNO	Purified Neem Oil
ENO	Epoxidized Neem Oil
ENOE	Epoxidized Neem Oil Ester

3.4 Fourier Transform Infrared (FT-IR) spectrometry

Conventional dispersive infrared (DIR) spectrometer uses grating monochrometer which contains within it a dispersive element. Dispersion occurs when energy falling on the entrance slit is collimated onto the dispersive element and the dispersed radiation is then reflected back to the exit slit, beyond which lies the detector. The dispersed spectrum is scanned across the exit slit by rotating a suitable component within the monochrometor, the two slits at the entrance and exit limit the wavenumber range of the radiation reaching the detector to one resolution width. Samples for which very quick measurement is needed cannot be studied because they cannot be scanned at speed. Unlike the DIR spectrometer, the Fourier Transform infrared (FTIR) spectrometer employs use of an interferometer, interference of radiation between two beams yield an interferogram, the interferogram is produced as a function of the change in path-length between the two beams. The two domains of distance and frequency are interconvertible by the mathematical method of Fourier transform (Stuart, 2004).

The FTIR has improved signal-to-noise ratio (SNR) per unit time, proportional to the square root of the number of resolution elements being monitored over the DIR

spectrometry (Fellgett's advantage). And, because in FTIR spectrometry the use of slit and other restriction device is not required, the total output of light can be passed through the sample continuously which results in a substantial gain in energy at the detector, hence leading to higher signals and improved SNR (Jacquinot's advantage), hence better quality of infrared spectra. The FTIR also have speed advantage over the DIR spectrometer, spectra is obtained on a millisecond time scale (Stuart, 2004).

In FT-IR spectrophotometer, the radiation absorbed by molecules of a sample is converted into energy of molecular vibration; the vibration is either stretching or bending. Stretchinginvolves rhythmic movement along band axis such that the interatomic distance is increasing or decreasing.And, bendingconsists ofa change in bond angle between bonds with a common atom. However, only vibrations that result in a rhythmical change in the dipole moment of the molecule are observed in IR spectrometry. Vibration spectra appear as bands rather than lines as a single vibrational energy is accompanied by a number of rotational energy changes. Band intensities are expressed either as transmittance (T); as ratio of the radiant power transmitted by a sample to the radiant power incident on the sample or absorbance (A); which is the logarithm to the base 10 of the reciprocal of the transmittance; $A = log_{10}(1/T)$. Intensities are reported in semi-quantitative terms of; vs=very strong, s=strong, m=medium, w=weak and vw=very weak Important areas for examination of the spectra are; 4000 to 1300cm^{-1} and 900 to 650cm^{-1}, it is called the functional group region. The intermediate region of 1300 to 900cm^{-1} is known as the fingerprint region (Silverstein*et al.,* 2005).

FTIR spectra were measured using Shimadzu-8400s FTIR Spectrophotometer in National Research Institute for Chemical Technology, Zaria. The sample holders were cleaned with

methanol and then with acetone thoroughly and a drop of the sample was placed on the measurement cell of the spectrometer. The sample was then scanned with infrared radiation through frequency range expressed as wave number of 4000 cm^{-1} to 500 cm^{-1} to obtain the spectra response. The amount of radiation absorbed by the sample was plotted against the wave number of the absorbed radiation. Each spike (absorption band) in the Infrared radiation spectrum represents absorption of energy.

3.5 Dynamic Viscosity Measurements

Dynamic viscosity is simply defined as the product of kinematic viscosity and density of a liquid. Dynamic viscosity of the sample was measured using Brookfield RVDV-I rotary Digital Viscometer shown in plate II.

Plate II: Measurement setup for Rheology Study with Brookfield Viscometer

The principle of operation of the Brookfield rotary viscometer is to drive a spindle that is immersed in a test fluid through a calibrated spring. The viscous drag of the fluid against the spindle is then measured by the spring deflection. The deflection of the spring

is measured by a rotary transducer, the measurement range of the viscometer (in milliPascal second) is determined by the rotational speed of the spindle, the size of the spindle, the shape of the spindle, the container in which the spindle rotates and the full scale torque of the calibrated spring. Viscosity is measured by the viscometer as a result of resistance experience by the spindle in rotating at a particular speed (in rotation per min) in the liquid. The viscosity range of a test fluid is inversely proportional to the size of the spindle and rotational speed. An appropriate spindle selection will result in measurement made between 20 to 80% of full measurement range.

- The oil was slowly introduced into the sample container of the viscometer using syringe so as to avoid air bubbles in the oil,
- The appropriate spindle was then selected and attached to the spindle connector. The sample container was then fit in place on the viscometer with the spindle immersed in it such that the groove on the spindle was covered completely in the oil sample in the sample container.
- The viscometer was adjusted such that the sample container was in thermal contact with water bath heated on a thermostatically controlled hot plate to vary the temperature of the sample within accuracy of ± 0.1℃ (see plate II). The temperature sensor was immersed in the water bath to monitor temperature. The bulb level on the viscometer was adjusted to ensure balance. About 30min was allowed for the oil in the sample container and the water in the container to be in thermal equilibrium at specific temperature value before readings were taken.
- Viscosities of the ENO and ENOE samples were made at rotational speed of 6 rpm using spindle zero. Spindle one was used for the PNO at rotational speed of 60 rpm.

The viscosity was measured within full measurement range of 20 to 80% and over temperature spectrum of 30 to 90°C within intervals of 10°C. Each measurement was taken three times and the average calculated for accuracy. A plot of viscosity against temperature was made to study the thermal behaviour of the liquid.

3.6 Construction and Calibration of Dielectric Liquid Test Cell

Cylindrical coaxial electrode test cell was constructed to host the fluid for measurements. Plate III show the test cell, the cell was constructed using Aluminium rod as the inner electrode and hollowAluminium pipe as the outer electrode. The electrodes were placed coaxial and concentric with one another mounted and glued on an insulating base material (see Appendix I for drawing and dimensions of the test cell).

Plate III: coaxial test cell

The test cell workssimplyas a capacitor. The two cylindrical electrodes act as charging plates and the space between them, dielectric medium. The measured capacitance by the test cell does not represent the true capacitance of the test cell, this is as a result of the effect of fringe on the capacitance introduced by the insulating base. The capacitance of air is calculated using the geometry of the test cell (see equation 3.2) and then subtracted from

the measured capacitance of the test cell with air as the dielectric and the remainder being the fringe capacitance as shown in equation 3.1, since the fringe capacitance does not change in value when the test cell is filled with aparticular sample, it is removed by subtracting from the measured capacitance of the sample considered.

$$C_{fringe} = C_{air\ measured} - C_{air\ calculated} \quad 3.1$$

the capacitance of the test cell when air is filling the space between the cylindrical electrodes is calculated from the geometry of the test cell using the following equation

$$C_{air\ calculated} = \frac{2\pi l\varepsilon_0}{\ln(b/a)} \quad 3.2$$

Where l is the length of the cylindrical electrodes in meter, m (they are of equal length), b is the inner radius of the outer cylinder and a, is the outer radius of the inner electrode all in meters, and C_{air} is the capacitance of air in pico-Farad, pF (Martinsen, 2011). And ε_0 is permittivity of free space and has value 8.8542×10^{-12} F/m.

The fringe capacitance once determined is subtracted from measured capacitance of a sample to obtain the true capacitance of the sample:

$$C = C_{sample\ measured} - C_{fringe} \quad 3.3$$

The relative dielectric constant of the sample is then calculated by dividing the true capacitance, C by the calculated capacitance with air as the filling medium.

$$\varepsilon_r = \frac{C}{C_{air\ calculated}} \quad 3.4$$

Errors introduced by the fringing capacitance have greatest effect when measuring samples with very low relative dielectric constant; the error diminishes as samples with higher relative dielectric constants are measured (Martinsen, 2011).

The test cell was calibrated using three different solvents; Toluene, methanol and acetonitrile as standard solution of known permittivity.The samples were introduced into the spacing between the electrodes using a syringe to avoid air bubbles. HM8118 LCR Bridge was then use to measure capacitance of the test solvents (Toluene, methanol and acetonitrile) at specific frequencies. The capacitance of toluene was measured at 100 Hz, methanol at 200 kHz and acetonitrile at 100 kHz.The positive terminal of the HZ184 cable to the LCR Bridge was connected to the outer electrode of the test cell and the negative terminal to the inner electrode. The measured value of capacitance was read and recorded from the display of the LCR Bridge. Equation 3.4 was then use to determine permittivity values of the test solvents. The test cell was cleaned after measurement using detergent and water then methanol and finally with dilute acetone.

3.7 Variation of Permittivity, Loss Tangent and Electric Conductivity of PNO, ENO, and ENOE with Frequency and Temperature.

3.7.1 Variation of Permittivity of the Samples with Temperature and frequency

HM8118 LRC Bridge with frequency response in the range of 20 to 200 kHz was used to vary frequency and measure values of capacitance. The LCR Bridge once connected to a device under test (DUT), measures the impedance and phase angle of the DUTdepending on the result, the component will be identified (since an idea capacitor, inductor and

resistor has loss angle of 0°, 0° and 90° respectively) and an internal equivalent circuit is created. The equivalent circuit represents the measurement circuit.

Two-electrode cylindrical coaxial dielectric test cell was used to host the sample (i.e the device under test). The cell was placed in an oven(heat chamber) whose temperature is controlled through a voltage source to vary the temperature of the heat chamber and it content (see plate iv). A thermometer was used to monitor the temperature of the heat chamber. Kevin clips attached to the HZ184 cable were used to clip the positive terminal to the outer electrode and the negative terminal to the inner electrode of the test cell. Capacitance of the oil sample considered was then measuredby pressing the C-D key of the LCR Bridge.The oven was maintained at fixed temperatures in the range of 20°C to 70°C. Thirty-five (35) frequency steps were selected within the range of 20 to 200 kHz. Frequency was adjusted by pressing the FREQ button and then the arrow button on the menu of the LCR Bridge. Readings of capacitance and dissipation factor were taken at each frequency value at fixed temperatures. The permittivity, ε_r of the samples were calculated using true measured capacitance of the fluids (the capacitance when fringe is removed) and the calculated capacitance of air with respect to geometry of the test cell (see equation 3.4). This enabled the understanding of the loss mechanism responsible for the conductivity of the fluid.

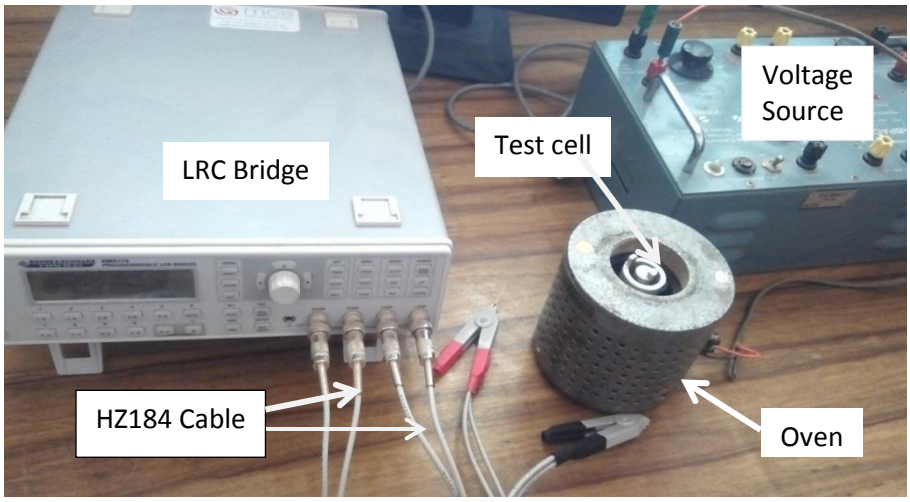

Plate IV: Experimental setup for frequency response and temperature dependency study of permittivity, loss tangent and electric conductivity

3.7.2 Variation of Loss tangent of the Samples with Temperature and frequency

The same experimental setup and procedure were followed as in 3.7.1 above. However, the loss tangent (dissipation) for the samples were measured and read directly from the LCR Bridge at frequencies range of 20 to 200 KHz and temperature range of 20 to 70°C.Measurementsof loss characteristics and Relative permittivity of the oil samples was carried out in accordance with the America Society for Testing and Measurement (ASTM) standard D924-92 procedures.

3.7.3 Variation of Conductivity with Frequency and Temperature

The conductivity of the samples at various frequencies and temperatures were calculated from the measured values of permittivity, loss tangent and frequencies steps considered using equation 2.31.

3.8 Simulation Using COMSOL Package

COMSOL Multiphysics is registered trade mark of COMSOL AB. COMSOL Multiphysics is a powerful interactive environment for modeling and solving all kinds of scientific and engineering problems. When solving the models, COMSOL Multiphysics uses the proven finite element method *(*FEM*)*. The software runs the finite element analysis together with adaptive meshing (if selected) and error control using a variety of numerical solvers. Partial differential equations (PDEs) form the basis for the laws of science and provide the foundation for modeling a wide range of scientific and engineering phenomena. COMSOL Multiphysics can be used in many application areas, for example: Bioscience, Diffusion, Chemical reactions etc. In creating mesh, COMSOL Multiphysics splits the domain into smaller sub-domains also known as primitive cells (as shown in plate v). The governing partial differential equations of the physics are then discretized and solved inside each of these primitive cells. The FEM gives an approximate solution, hence the finer the mesh the higher the accuracy of the approximate solution.

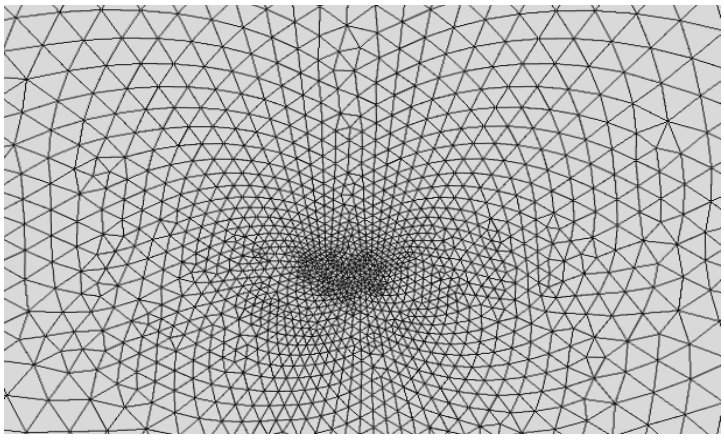

Plate V: Extra fine mesh around tip of the high voltage point electrode

3.8.1 Simulation Procedure

In the study of pre-breakdown mechanisms, there are number of geometries considered. Even though most part of high voltage equipment have quasi-uniform field, the easier configuration use for pre-breakdown study is the point-plane geometry with divergent field. In this work, three different electrode geometries that are present in real power equipment were simulated (see figure 3.1). These include; Point to plane electrode gap, Rod to plane with Kraft paper, and Elevated rod geometriesadapted from Berg and Lundgaard(1999).

Construction of Geometrical Models: In the point to plane electrode gap configuration, the tip radius was set to 30 μm, and the point electrode 15 mm long, a 0.7 mm gap was maintained for the first measurement and then varied to 2.5 mm. The ground electrode in all the configurations was constructed of the same dimension; 110 mm long and 5 mm height. The paper insulation was constructed from a rectangle of 110 mm width and 1 mm height. The high voltage electrode in both the Rod to plane with Kraft paper and Elevated rod configuration was constructed from a rectangle of height 23mm and width 10mm. The effect of microbubbles of air and water on electric field distribution at high field regions was studied by constructing air and water micro bubbles of various radii and positioning them around high field regions. In the point to plane geometry three micro air and water bubbles were simulated with circles of radius 50 μm, 60 μm and 70 μm for each simulation case (i.e. air and water). And, in the rod to plane geometry, micro air bubble were constructed from two circles of radius 80 μm and 140 μm, same dimension were maintained for the case of water bubbles. Finally, in the Elevated rod geometry, micro air bubbles (two) of radius 130 μm (each) and a 90 μmradius circle was simulated in the high

field region. PNO was used as natural insulating fluid. Same simulations were carried out using and transformer oil as the insulating fluid and the results compared.

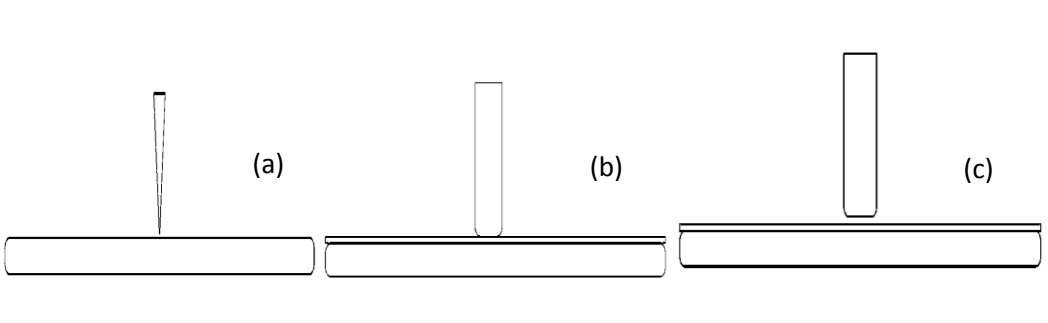

Figure 3.1: Geometric models of (a) Point to plane, (b) Rod to plane, And (c) Elevated rod

The following steps were observed in creating the model;

- The model environment was setup in 2D and in unit millimetre.
- Then geometric objects were created.
- Materials were selected from the Material Library and material properties specified.
- Electrostatics was selected from the AC/DC Module as the appropriate physics module for the simulation and the appropriate boundary conditions specified
- Extremely fine mesh was selected as the appropriate mesh type.
- The base electrode was grounded, and voltages within the range of 1 kV to 10 kV were applied to the high voltage electrode. The permittivity of the impregnated Kraft paper was set as 4.7, and plots of electric field distribution in the different geometric models were made and analysed.

3.8.2 Estimation of Permittivity of oil impregnated Kraft-paper

Kraft paper was used as paper insulation in the simulation. Kraft-paper is made of cellulose fibre hence, it has permittivity, $\varepsilon_{Fibre}$of 5.0. When Kraft-paper is immersed in oil (PNO,

ENO or ENO), its permittivity changes. The permittivity of Kraft paper sucked with PNO,$\varepsilon_{impregneted\ Kraft-paper}$ was determined using the following equation;

$$\varepsilon_{impregneted\ Kraft-paper} = \varepsilon_{Fibre}\left[1 - K^2\left(\frac{1}{1+K\left(\frac{\varepsilon_{Fibre}}{\varepsilon_{Oil}}-1\right)}\right)\right] \quad 3.5$$

where,ε_{Oil} is permittivity of oil and equals 3.5 for PNO and is 2.2 when transformer oil is used, K is determine from the volume of the oil and Kraft paper;

$$K = \sqrt[3]{\frac{V_{oil}}{V_{Kraftpaper}}} \quad 4.1$$

assuming 1.2 g/cm^{3}density of Kraft paper, K equals 0.45 (Martin *et al.*, 2007).

CHARPTER FOUR

RESULTS AND ANALYSIS

4.1 Fourier Transform Infrared Spectrometry of the Synthesized Samples

The FTIR Spectrum of the PNO, ENO, and ENOE is as shown in the figures 4.1, 4.2 and 4.3 respectively. The assignment of the peaks and mode of vibration that resulted in the peaks are shown below in table 4.1 for the three samples.

Table 4.1: FTIR spectra assignment and mode of vibration for the three samples

Frequency cm^{-1}	Mode of vibration	Relative intensity		
		PNO	ENO	ENOE
2928	C-H asymmetric stretching vibration of CH_2	vs	vs	vs
1740	C=O stretching vibration	vs	vs	vs
1660	C=C stretching vibration	w	none	none
1450 1455 1453	C-H Scissoring vibration of CH_2 and CH_3	m	m	m
1366 1370 1357	C-H symmetrical bending vibration of CH_3	w	m	m
853	Asymmetric ring stretching vibration of C-C during contraction of the C-O	none	none	w
719 730 728	C-H rocking vibration of CH_2	m	m	m

Key: vs=very strong, s=strong, w=weak and m=moderate/medium

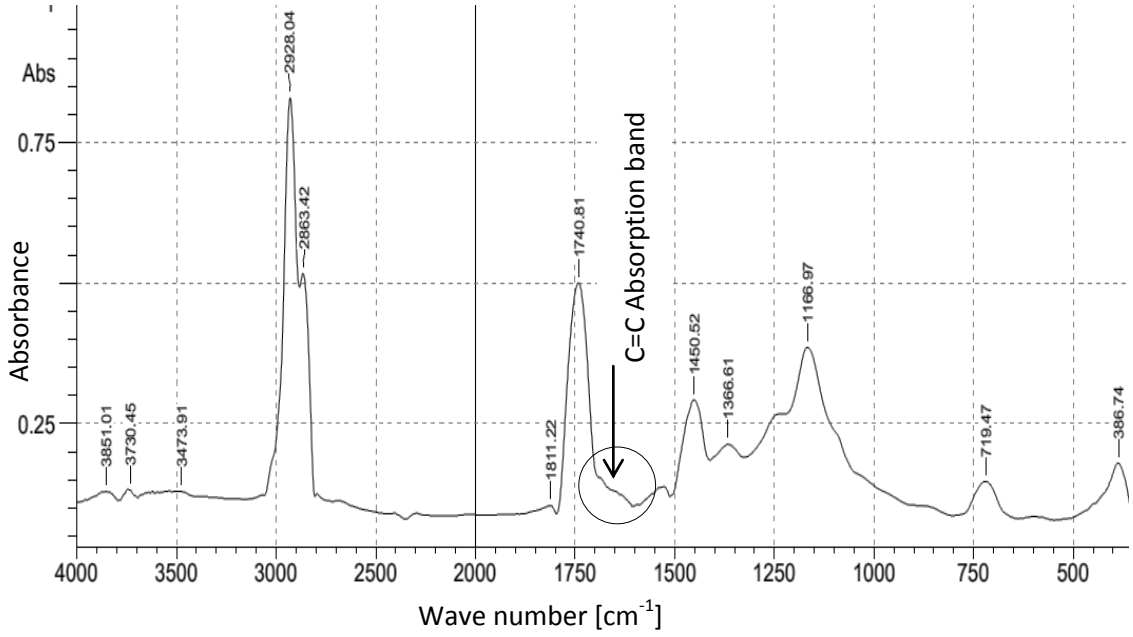

Figure 4.1: FTIR Spectrum of purified Neem Oil (PNO)

The circular mark on figure 4.1 shows carbon-carbon double (alkene) bond absorption band. Vibrations resulting from carbon-carbon double bonds have absorption energy in frequency range of 1680 to 1600 cm^{-1} (Stuart, 2004). In contrast with circles on figures 4.2 and 4.3, the carbon-carbon absorption band as seen in figure 4.1 is absentin the ENO and ENOE spectra.

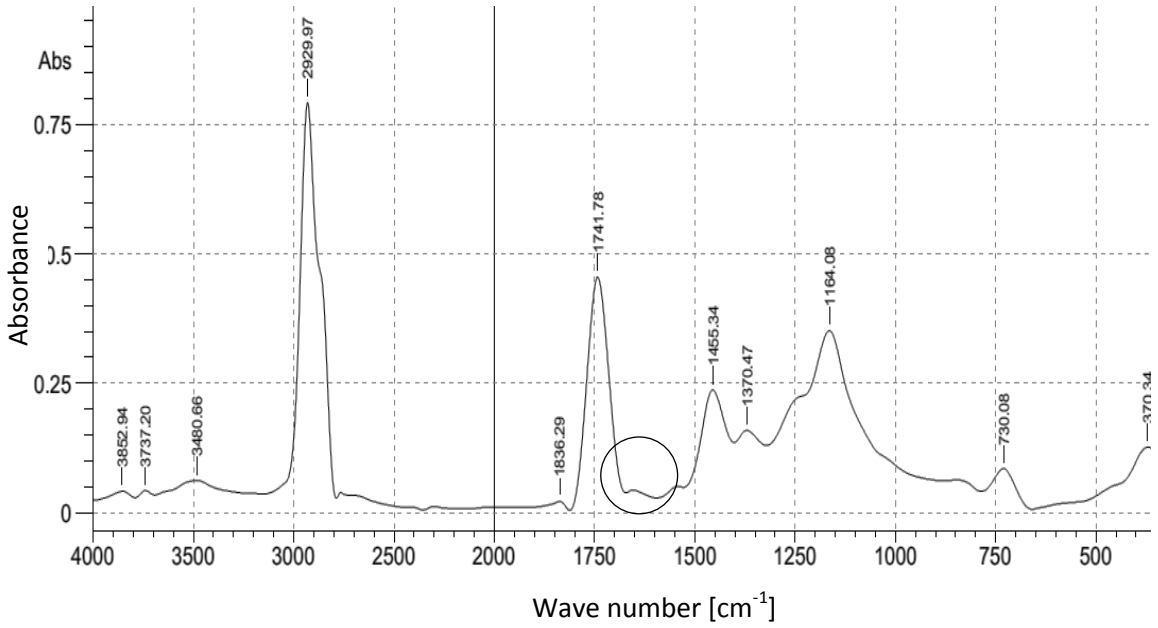

Figure 4.2: FTIR Spectra of Epoxidized Neem Oil (ENO)

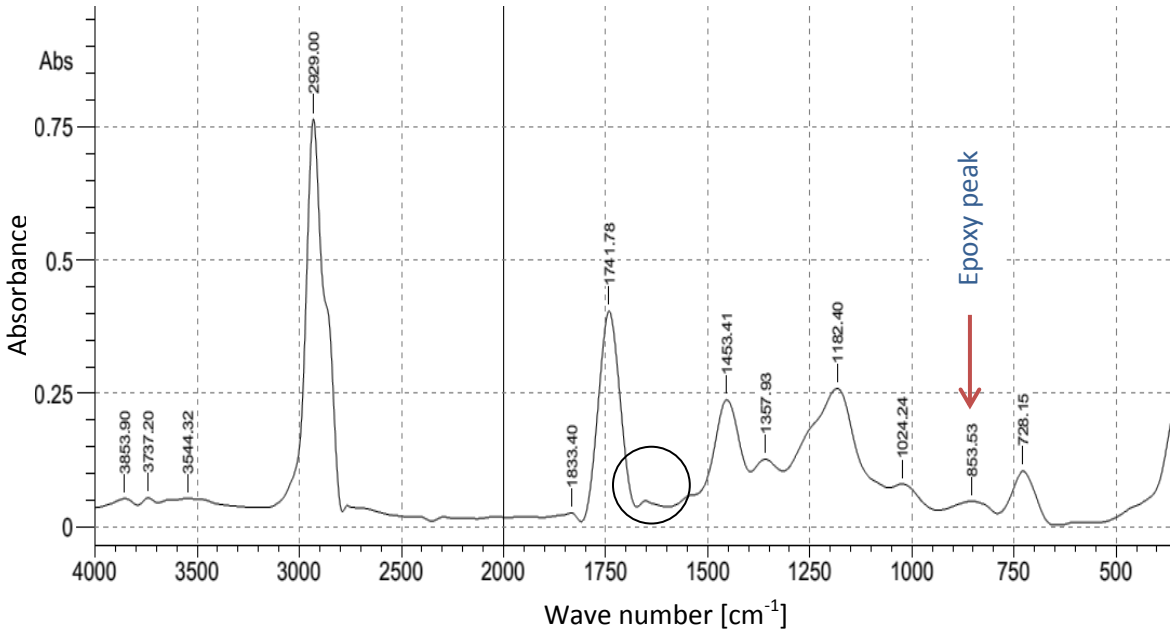

Figure 4.3: FTIR Spectra of Epoxidized Neem Oil Ester (ENOE)

The absence of the carbon-carbon absorption band in both the ENO and ENOE is as a result of conversion of the double bonds in the PNO in an epoxidation reaction. Chemical modification was effective in converting unsaturation presents in some of the fatty acids in the purified and transesterified sample. The observed broad peak in ENOE sample in figure

4.3 within the lower region of the spectrum (853 cm^{-1}) is due to the presence of epoxy functional group. The epoxy finger prints appears around peaks at 844 and 829 cm^{-1} (Abdelmalik *et al*., 2014), this confirms the conversion of unsaturation in the oil to epoxide. Peaks at 719, 730 and 728 cm^{-1} in figure 4.1, 4.2 and 4.3 respectively is as a result of methylene rocking (bend) vibration of CH_2 in which all methylene groups of straight chain alkanes in the samples vibrate in Phase. The epoxy peak is pronounced in ENOE compared with ENO. This may be because the epoxy group of ENO is buried in the triglyceride.

4.2 Dynamic Viscosity of the liquid samples

The dynamic viscosity of the samples measured at temperature of 30°C and atmospheric pressure is presented in table 4.2;

Table 4.2 Dynamic Viscosity of the samples at 30°C

Sample(s)	Dynamic Viscosity (Pa.s)
PNO	0.081
ENO	0.947
ENOE	0.664

The viscosity of the purified neem oil (PNO) was measured to be 0.081 Pa.s. Chemical modification was observed to have significant effect on the rheology of the oil. When the sample was passed through epoxidation to produce (ENO), the viscosity increased to 0.947 Pa.s. Transesterification of ENO to produce ENOE was observed to have reduced

the viscosity to 0.664 Pa.s. The viscosity of the epoxy ester of neem oil falls between the viscosity of the purified neem oil and epoxy neem oil. Comparison of the viscosity of the samples with that of FR3 natural ester fluid in Table 4.3 shows that PNO has similar rheology property with FR3 while ENO and ENOE have much higher viscosity compared to FR3. The change in viscosity of the oil samples with respect to temperature is shown in Figure 4.4. There is systematic decrease in viscosity of all the samples with increasing temperature.

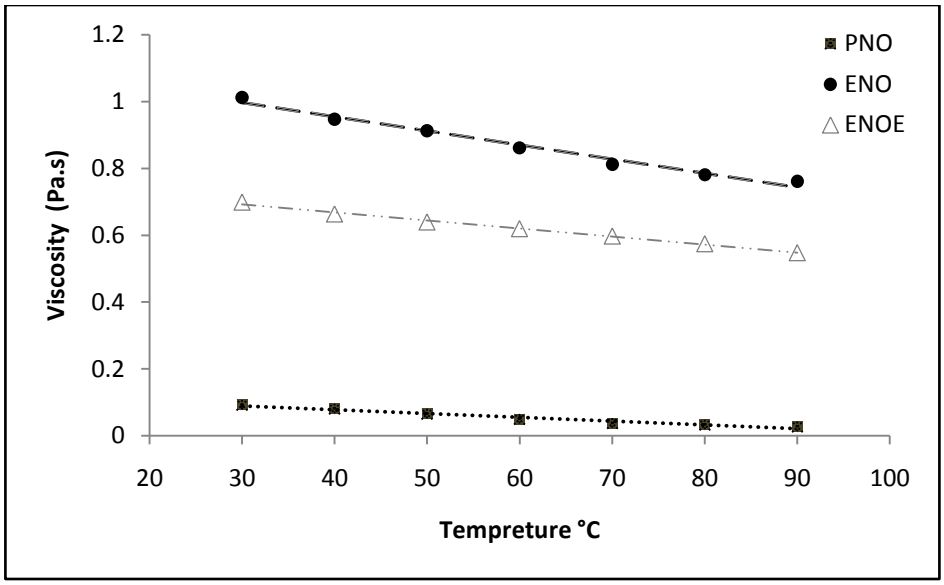

Figure 4.4: Temperature dependency of dynamic viscosity

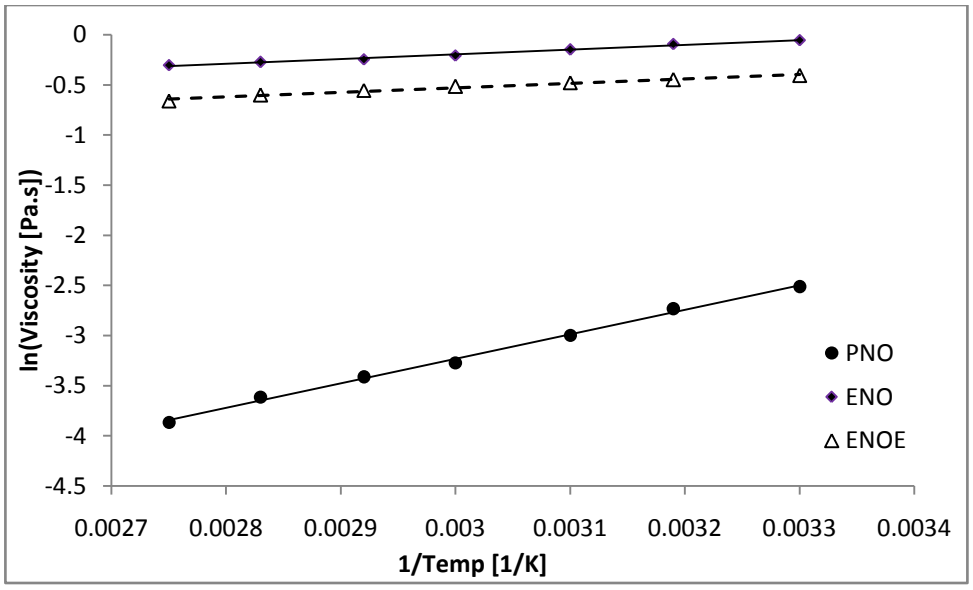

Figure 4.5: Arrhenius plot for the dynamic viscosity of the samples

The samples show similar Arrhenius behaviour in the temperature range considered. Increase in temperature (heat gain) results to increase in kinetic energy (mobility) of the

molecules of the samples consequently leading to reduced resistive force acting between layers of the samples. The activation energies of the samples were determined from the Arrhenius plot (figure 4.5), from the calculated slopes. The straight lines fit on the data points with correlation coefficient (R^2) of 0.9965, 0.9884 and 0.9815 for the PNO, ENO and ENOE samples respectively. The Arrhenius plot of the viscosity-temperature relation shows that the sample with higher viscosity has high activation energy. This implies that the higher the viscosity, the more the energy required to reduce the resistive force acting between the layers of the liquids.

Table 4.3: Properties of seed oils

Sample(s)	Activation Energy (eV)	Dynamic Viscosity (Pa.s)	
		At 30°C	At 60°C
PNO	0.21	0.081	0.038
ENO	0.041	0.947	0.812
ENOE	0.038	0.666	0.598
FR3	-	0.086	0.022

The viscosity of the FR3 as presented (at 30°C) is measured at 20°C

4.3 Calibration of the test cell

The capacitance of air, was calculated from the geometry of the test cell as 4.5302 pF using equation 3.2. Table 4.2 show correlation between measured permittivity by the test cell and literature values of permittivity of the test solvents. Literature values were obtained from Louisiana state university Macromolecular studies group server (Dielectric constants of solvents, 2014).

Table 4.4: calibration of the test cell

Solvent	Measured Permittivity	Literature value of permittivity	Percentage Error
Toluene	2.38	2.38	0.21%
Methanol	34.9	32.7	6.3%
Acetonitrile	37.2	37.5	0.81%

4.4 Dielectric Dispersion of the samples

A semi-log and log-log plot of relative permittivity against frequency of the three samples is as shown in figure 4.6 and 4.7 respectively, the three samples show same pattern of frequency dependency. Resonance was observed at 50 Hz which is suspected to be due to interference with the power frequency. Similar to viscosity behaviour, the relative permittivity of the sample changes with chemical modification. PNO has relative permittivity of 3.59 at 60 Hz while ENO and ENOE have relative permittivity of 5.87 and 4.63 respectively at the same frequency.

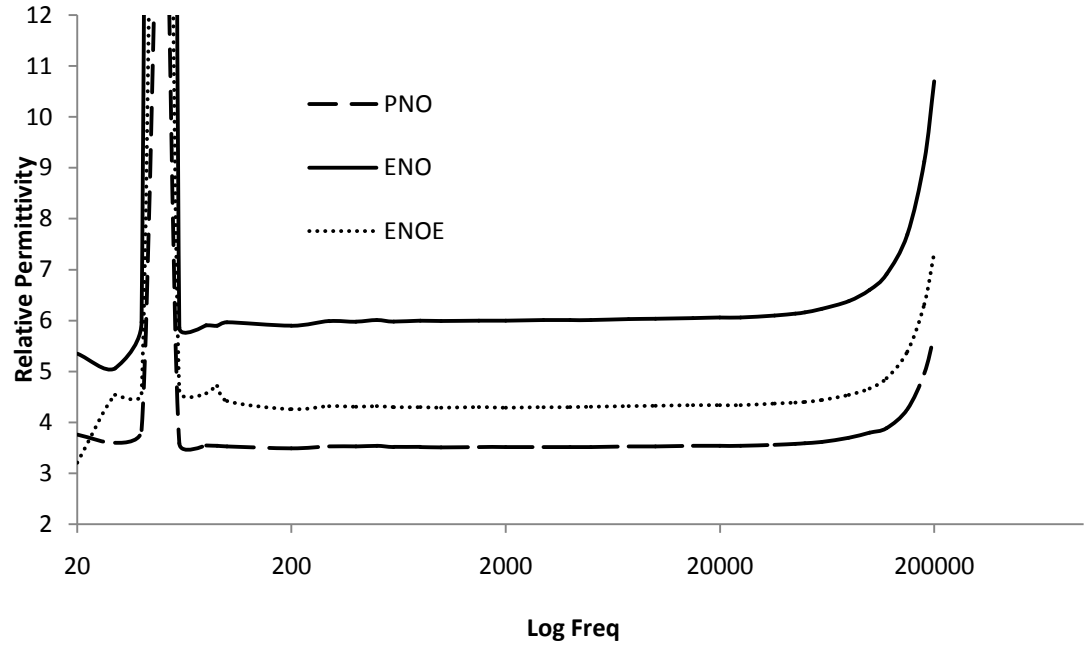

Figure 4.6: Semi-log plot of Permittivity against frequency of the three samples at 20°C

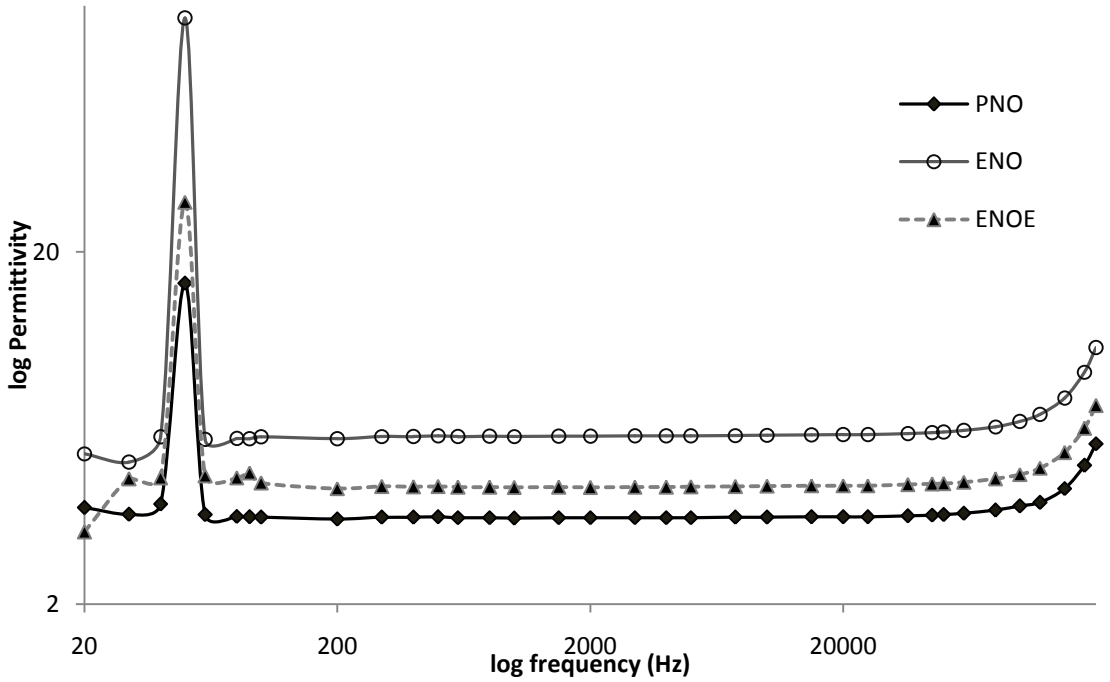

Figure 4.7: Dispersion curve of the three samples

4.4 Frequency-Temperature Dependency of the Loss Tangent

A log-log plot of loss tangent as function of frequency and temperature were made as shown in the figures 4.8, 4.9 and 4.10. Similar to the observation while measuring relative permittivity, there issharp increase in loss tangent at 50 Hz. The loss tangent between the frequencies of 15 Hz to 15 kHz shows a linear relation. The slope of the lines in the region is -1, implying inverse relationship between loss tangent and frequency. The loss tangent is observed to increase with increase in temperature. At frequencies greater than 15 kHz, loss tangent in the samples increased with increase in frequency.

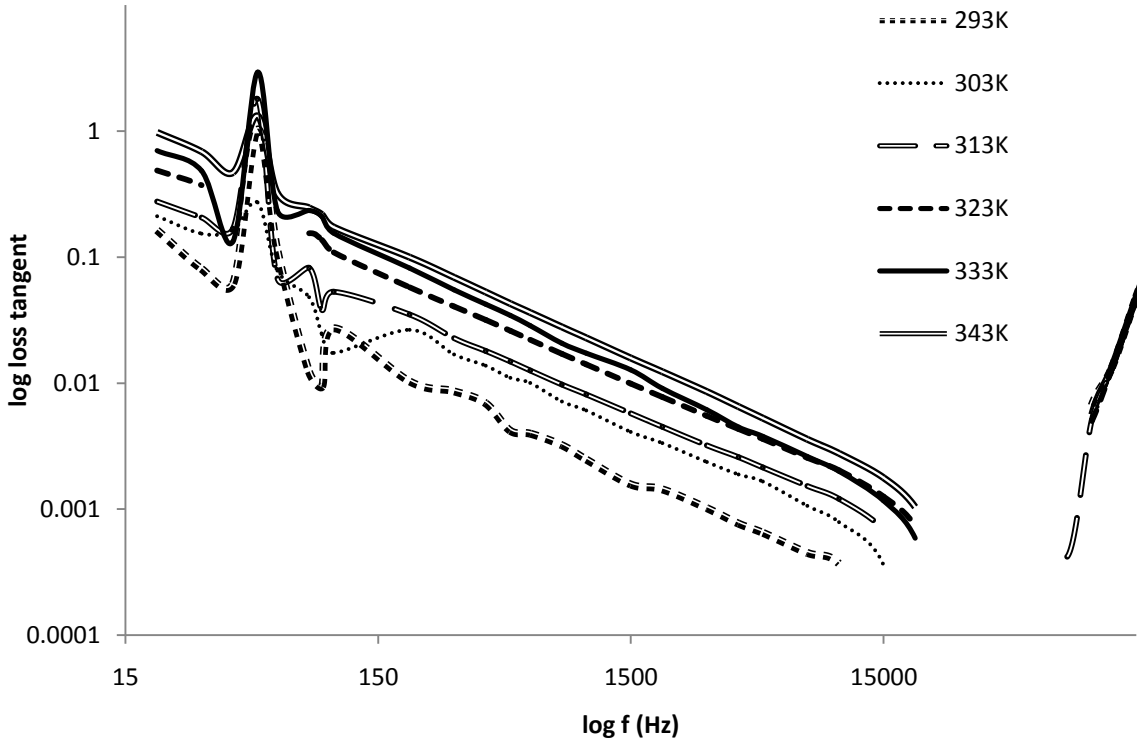

Figure 4.8: A log-log plot of loss tangent against frequency for Neem Oil (PNO) Sample at temperature range of 293K-343K

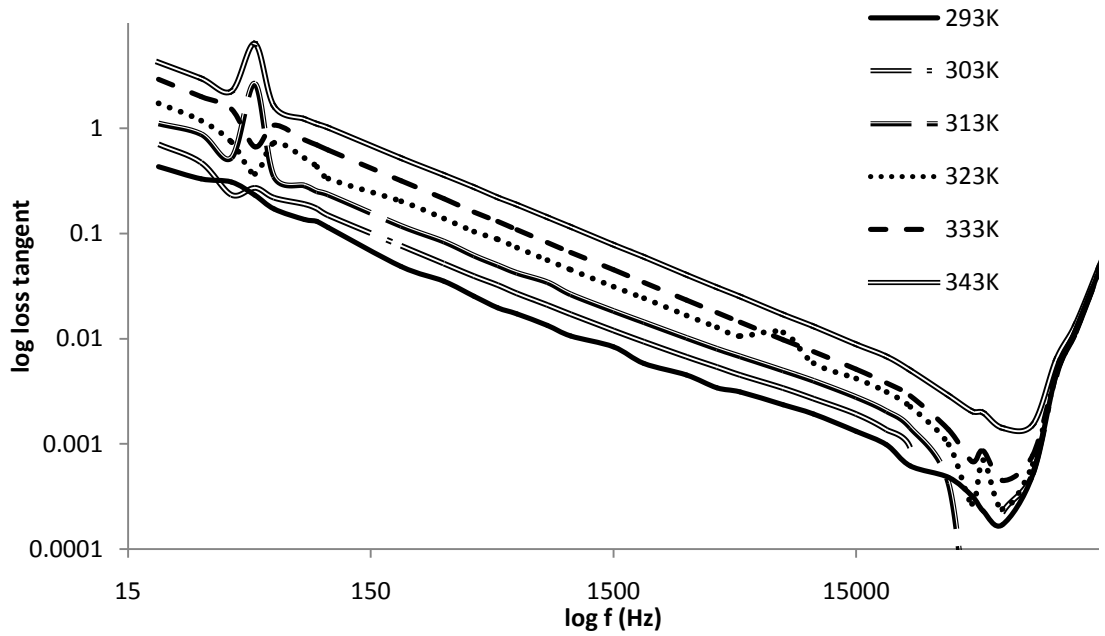

Figure 4.9: A log-log plot of loss tangent against frequency for Epoxidized Neem Oil (ENO) at temperature range of 293K-343K

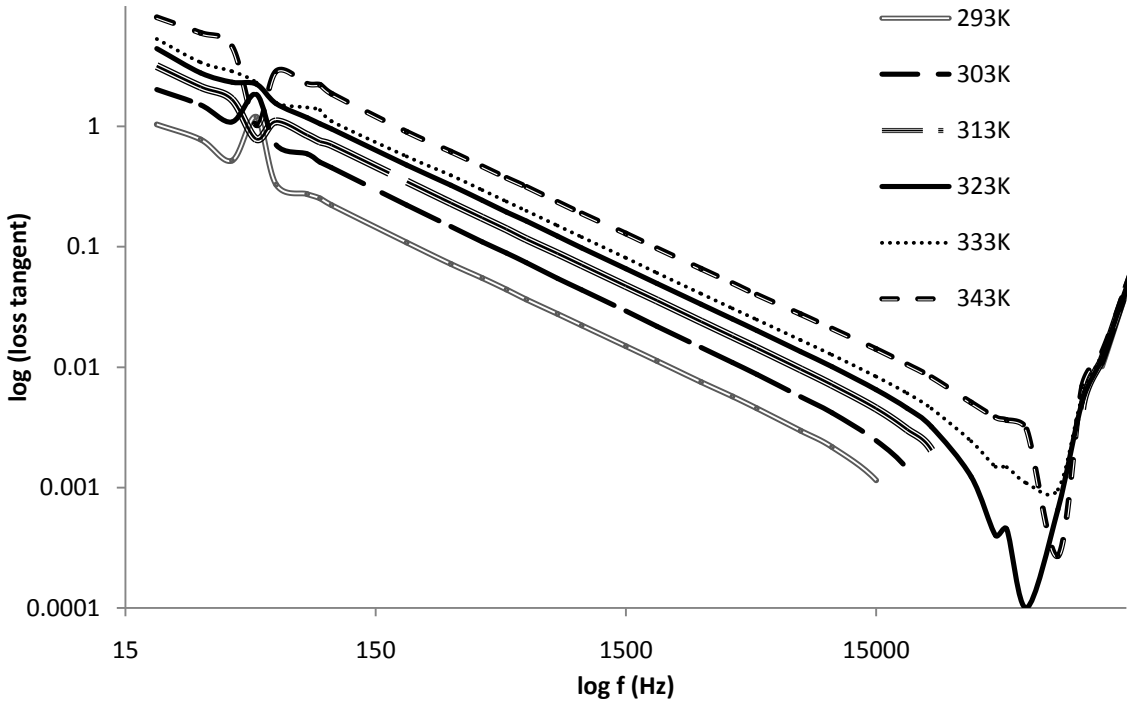

Figure 4.10: A log-log plot of loss tangent against frequency of epoxidized Neem Oil Ester (ENOE) Sample at temperature range of 293K-343K

4.5 Frequency-Temperature Dependency of Electric Conductivity

Figure 4.11 is a composite semi-log plot of ac conductivity against frequency of PNO, ENO and ENOE samples. Log-log plots of conductivities as a function of frequency at fixed temperatures for the PNO, ENO and ENOE samples is represented by figures 4.12, 4.13 and 4.14 respectively. The conductivity is only weakly dependent on frequency in the range of 20 Hz to 15 kHz, only increasing slightly with frequency variation in this range. However, beyond 15 kHz, the conductivity is observed to increase rapidly with increase in frequency. Peaks at 50 Hz could be a result of resonance in the equivalent circuit of the LCR Bridge used or due to impulse resulting from noise interference of electrical equipment in the Laboratory with power frequency (50 Hz).

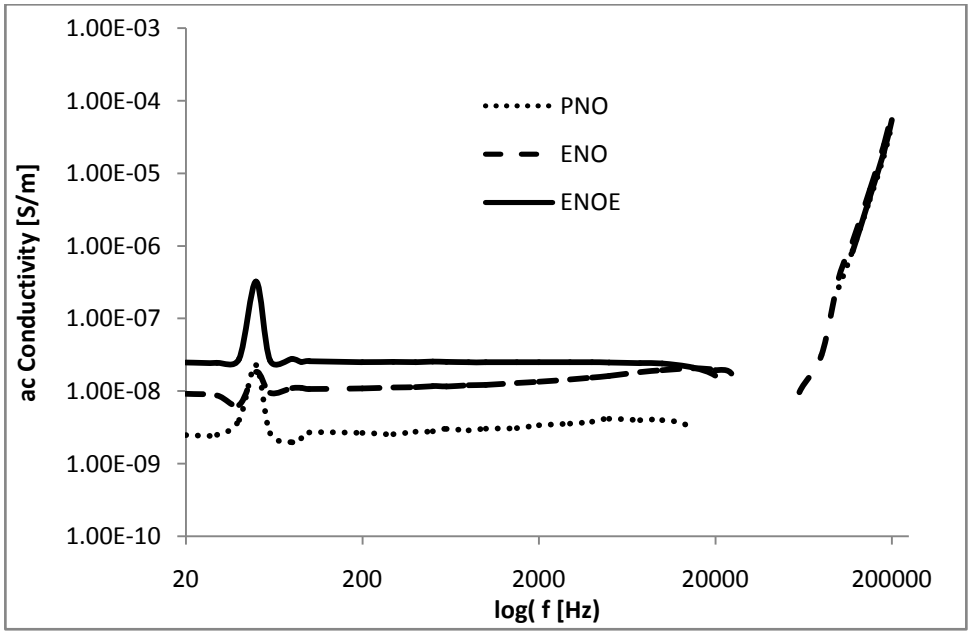

Figure 4.11: ac conductivity against log of frequency for PNO, ENO and ENOE at temperature of 30°C

As seen in figure 4.11, ac conductivity of the samples increased with processing with PNOhaving least conduction and ENOEhaving the greatest conductivity. Decrease in

viscosity of the ENO when transesterified led to increase ac conductivity in the ENOE sample.

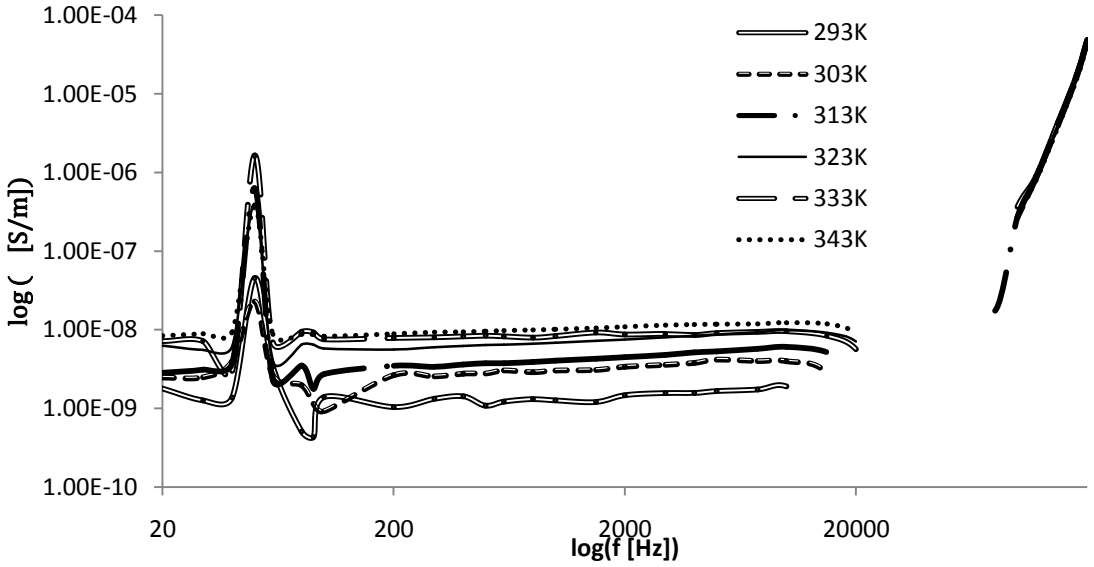

Figure 4.12: A log-log plot of electrical conductivity against frequency for Neem Oil (PNO) Sample at temperature renges between 293K-343K

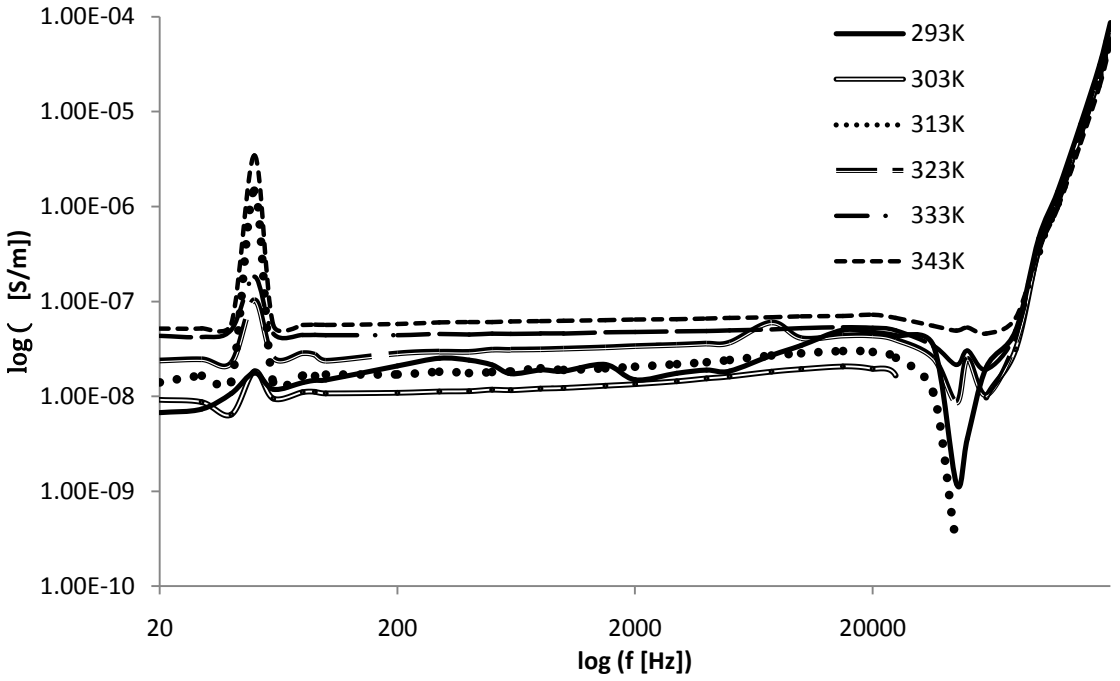

Figure 4.13: A log-log plot of electrical conductivity against frequency of Epoxidized Neem Oil (ENO) Sample at temperature range of 293K-343K

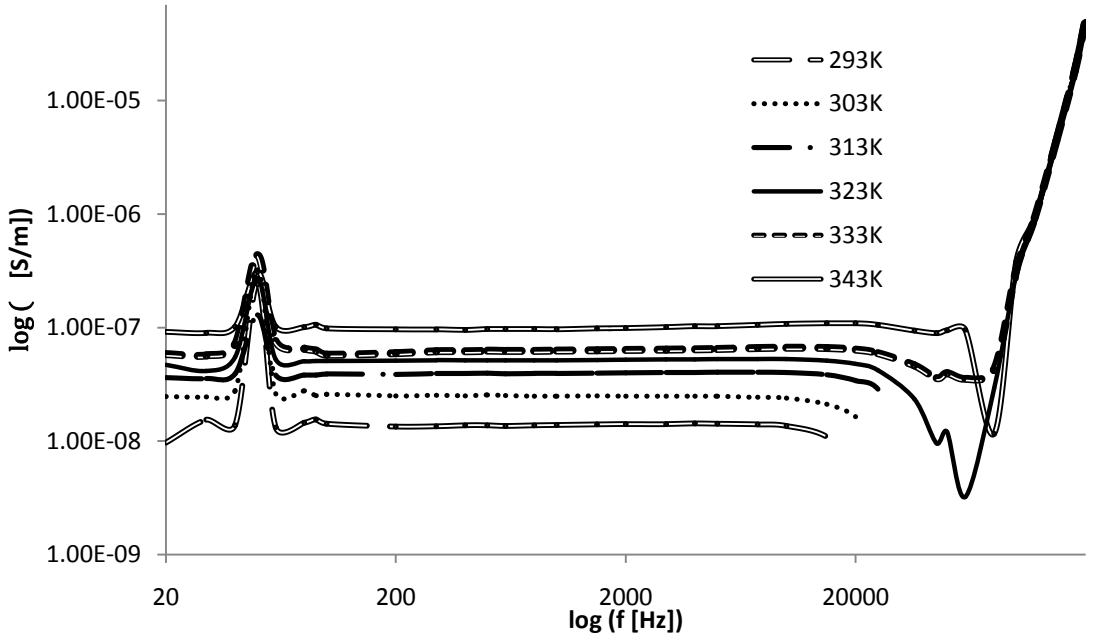

Figure4.14: A log-log plot of electrical conductivity against frequency of epoxidized Neem Oil Ester (ENOE) Sample at temperature range of 293K-343K

4.5.1 Temperature dependence of electric conductivity

The ac conductivity of the PNO, ENO and ENOE samples at frequency of 60 Hz is plotted against temperature as shown in figure 4.15.The electric conductivity is evaluated from the frequency response data of the samples within temperature range of 20°C to 70°C. The plot shows an increase in electrical conductivity with increase in temperature.

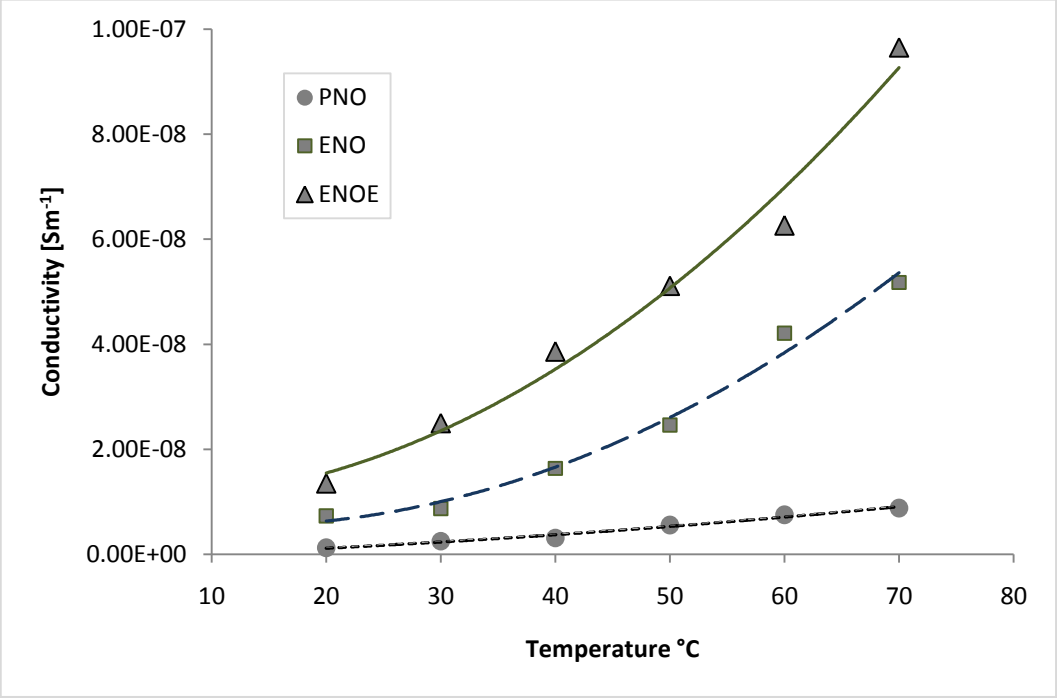

Figure 4.15: Temperature dependence of electrical conductivity at 60 Hz

Arrhenius plot (figure 4.16) was made so as to determine activation energies of the samples. ac conductivity was on Arrhenius axes (i.e. the vertical) as presented in figure 4.15. The activation energies of the samples were determined from the slope of the Arrhenius plot 4.15 and the relation;

$$\sigma_{AC} = \sigma_0 \exp(-E_a/KT) \qquad 4.1$$

where σ_0, the pre-exponential factor is the dc conductivity in Siemen per meter (Sm^{-1}), E_a is the activation energy in electron volt (eV), K is Boltzmann constant (8.6173×10^{-5} eV) and T is temperature in Kelvin (K) (Saroj and Singh, 2012).

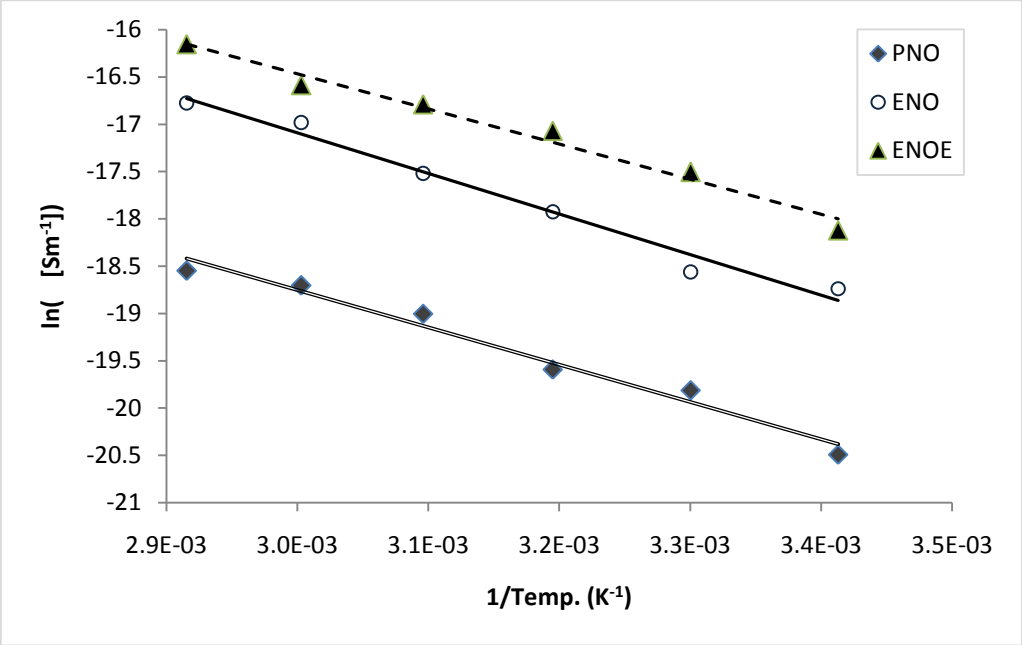

Figure 4.16: Arrhenius plot of the ac conductivity for the three samples

Table 4.5: measured parameters at 20°C and 60Hz

Sample	tan δ	Permittivity	AC Conductivity (Sm^{-1})	Activation Energy for σ_{AC} (eV)
PNO	0.11146	3.50	1.26×10^{-9}	0.34
ENO	0.23066	5.87	7.30×10^{-9}	0.37
ENOE	0.32805	4.63	1.35×10^{-8}	0.32

The Arrhenius type equation for electrical conductivity (equation 4.1) fit the data in figure 4.15 with correlation coefficients (R^2) of 0.9747, 0.9795 and 0.9803 for the PNO, ENO

and ENOE respectively. Table 4.4 shows values of the activation energies for the conductivity of the three samples. The PNO sample has activation energy of 0.34 eV, after epoxidation, the activation energy increased to 0.37 eV andthe ENOE sample hasactivation energy of 0.32 eV. Also shown are values of permittivity, loss tangent and acconductivity of the samples as determined at same temperature and frequency. A comparison of the electric conductivity in the three samples (*table 4.4*) show that PNO is the least conducting with the ENOE sample having the greatest conductivity.

4.6 Simulation of Discharge Development in Insulation System with the Oil

4.6.1 Point to Plane Gap Electrode Configuration

The potential between the tip of the high voltage electrode and the ground is represented by the plot as a function of distance. The potential is maximum at the electrode tip and decreases toward the ground electrode. From plate vi, it is seen that electric field is maximum just at the tip of the high voltage electrode and decay as square of the distance with the ground electrode. Much work would be done in moving a charge in the field just around the tip than in the field just near the surface of the ground electrode. Electric potential is inversely proportional to distance. That reveals that sharp edges in a high voltage device are prone to high field enhancement and that is the region where activities such as partial discharges that could cause insulation degradation and eventual breakdown of the system.

Figure 4.18 shows that variation of electric field from the tip to grounded electrode. Field strength of about 2.3×10^6 was observed around the tip. This field decreased exponentially as you move close to ground electrode.

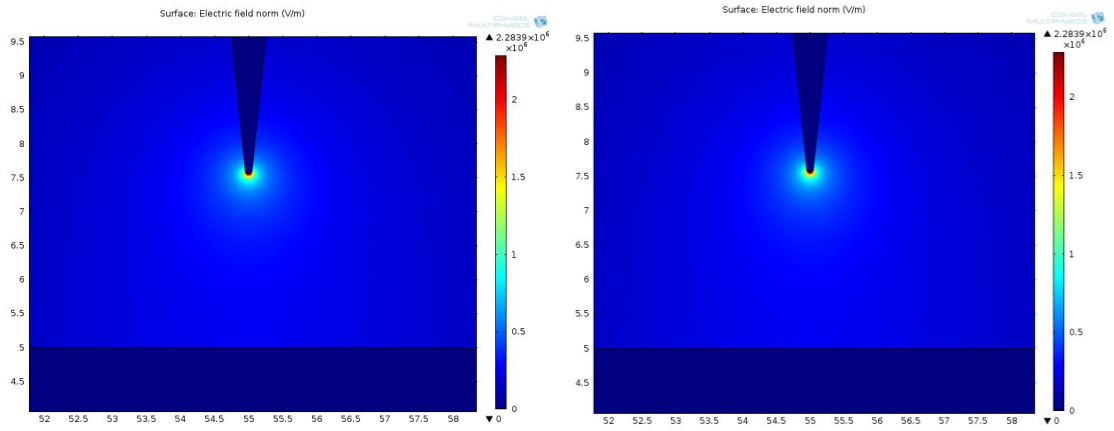

Plate VI: Electric Field distribution in the point-plane electrode at applied voltage of 1 kV (a) in Natural Ester Fluid, and (b) in Transformer oil

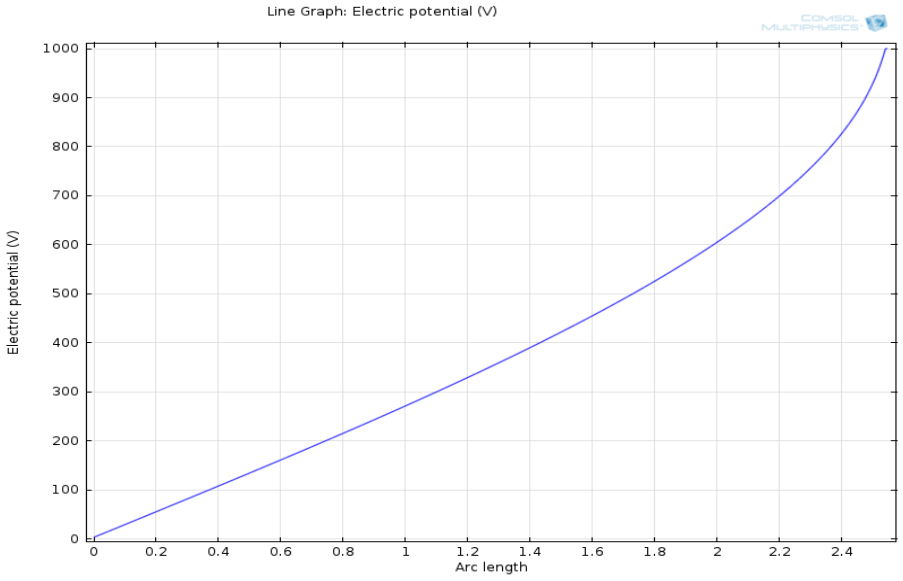

Figure 4.17: Variation in electric potential field between the tip of the high voltage electrode and the ground at applied voltage of 1 kV

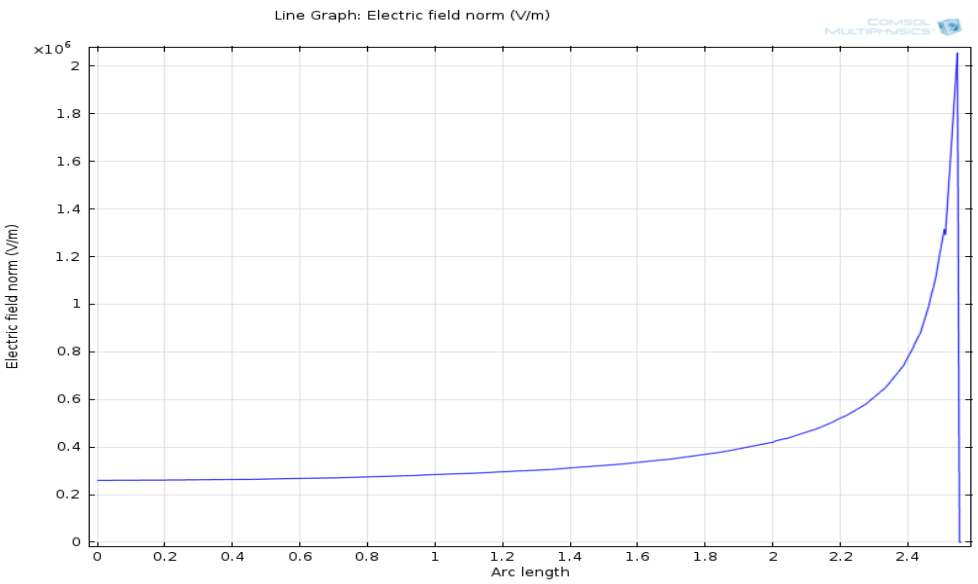

Figure 4.18: Variation of Electric field with distance between the tip of the high voltage electrode and the ground at applied voltage of 1 kV

Table 4.6: correlation between applied voltage and maximum electric field in the point to plane geometric model

S/No	Applied Voltage (kV)	Maximum Electric Field (kV/mm)			
		At arc length of 2.5mm		At arc length of 0.7mm	
		Seed Oil	Mineral Oil	Seed Oil	Mineral Oil
1	1.0	2.30	2.30	4.50	4.50
2	2.0	4.60	4.60	9.00	9.00
3	4.0	9.10	9.10	18.0	18.0
4	6.0	13.7	13.7	25.0	25.0
5	8.0	18.3	18.3	35.0	35.0
6	10.0	22.8	22.8	45.0	45.0

Comparing field distribution in mineral oil and the ester, there is no difference in the field strength in in the oil samples.

4.6.2 Rod to Plane electrode Configuration

As the geometric model is symmetrical about the y-axis hence only half of the physical model is shown. The field in concentrated at the triple region where the rod, solid insulation and the oil meet. The difference in the field distribution in the two oil samples is clearly seen in Platevii.

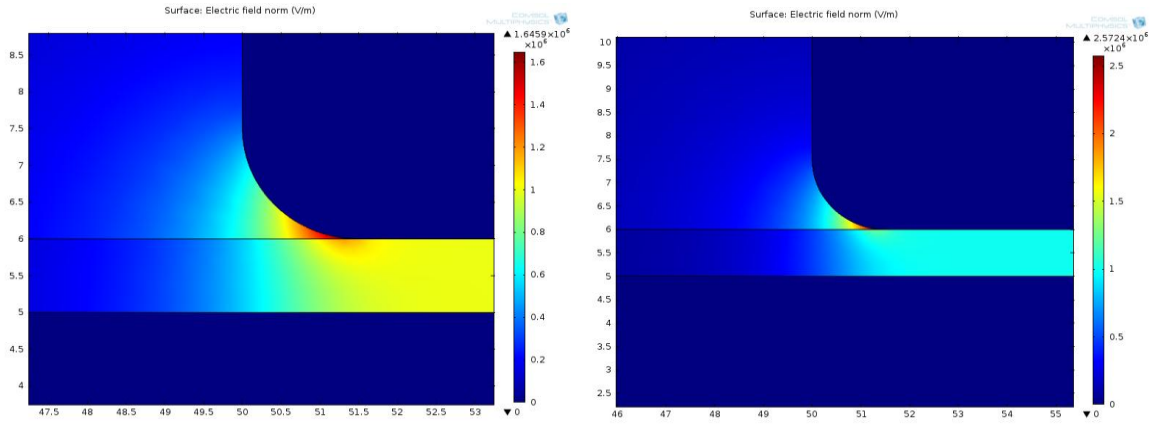

Plate VII: Electric field distribution at triple junction at applied voltage of 1kV (a) using natural ester fluid as insulating fluid (b) using transformer oil as insulating fluid

Table 4.7 correlation between applied voltage and maximum electric field in the rod to plane geometry

S/No	Applied Voltage (kV)	Maximum Electric Field (kV/mm)	
		Natural Ester Fluid	Transformer Oil
1	1.0	1.60	2.50
2	2.0	3.00	5.00
3	4.0	6.00	10.0
4	6.0	9.00	15.0
5	8.0	12.0	20.0
6	10.0	16.0	25.0

A linear relationship between the applied voltage and maximum electric field produced exist and is plotted in figure 4.19. The field strength in the mineral oil is higher than that of the natural ester. That is an indication that under similar conditions, the insulation paper impregnated with natural has higher breakdown strength compare with mineral oil impregnated paper. This is in line with previous report on breakdown strength of natural ester-impregnated paper.

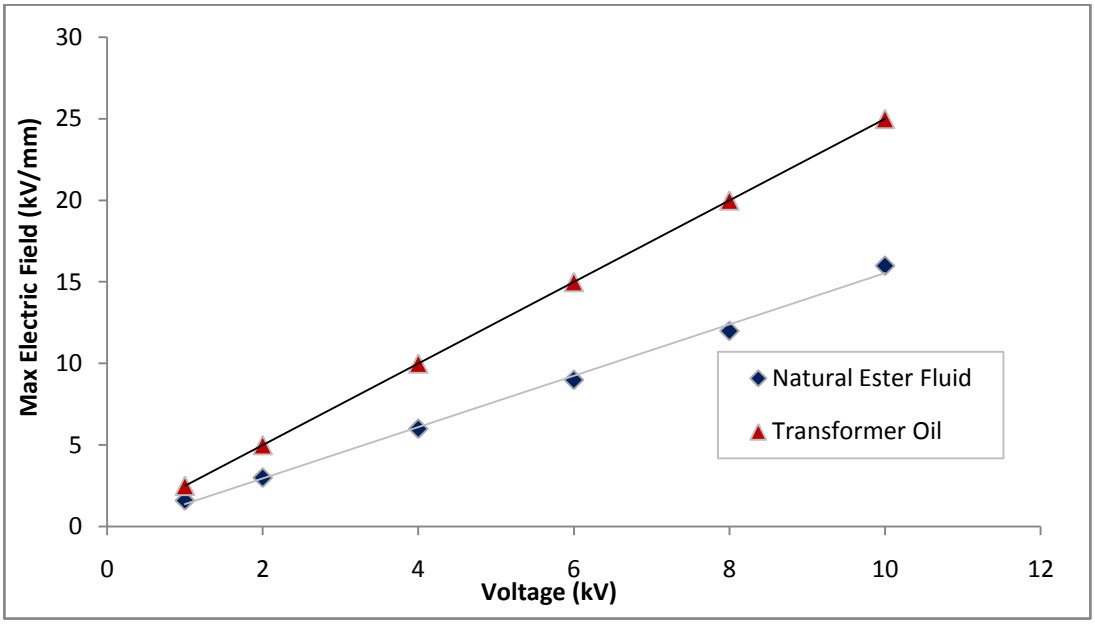

Figure 4.19: Relationship between Applied voltage and maximum electric field in rod to plane configuration

4.6.3 Elevated Rod Geometric Model

In the elevated rod geometry, there is oil in between the rod and impregnated paper lying on top of the grounded electrode. The field distribution in this configuration is as shown in plate viii, for the same applied voltage the maximum electric field produced is seen to be more intense in the transformer oil than in the natural ester fluid.

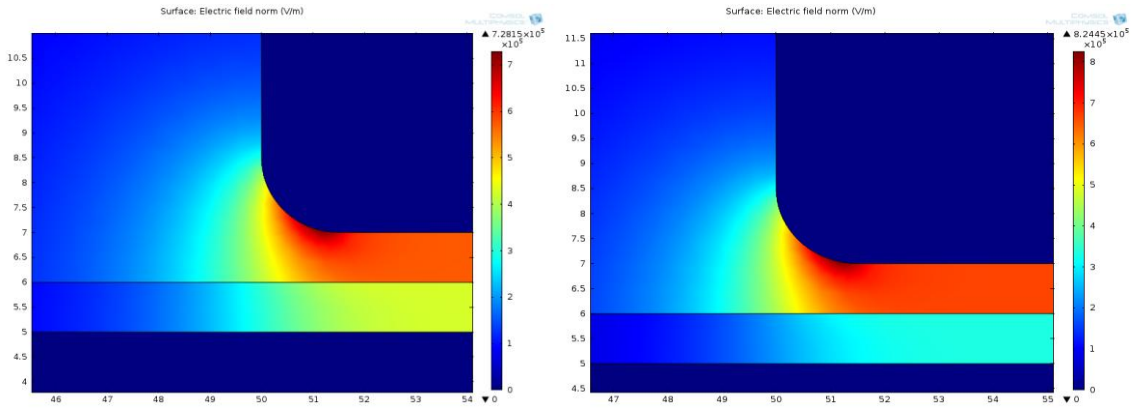

Plate VIII: Electric field distribution in elevated rod geometry at an applied voltage of 1kV (a) in Natural Ester Fluid (b) in Transformer Oil

Table 4.8 Correlation between applied voltage and maximum electric field in the elevated rod configuration

S/No	Applied Voltage (kV)	Maximum Electric Field (kV/mm)	
		Natural Ester Fluid	Transformer Oil
1	1.0	0.7	0.8
2	2.0	1.4	1.6
3	4.0	2.5	3.3
4	6.0	4.0	4.9
5	8.0	5.0	6.6
6	10.0	7.0	8.2

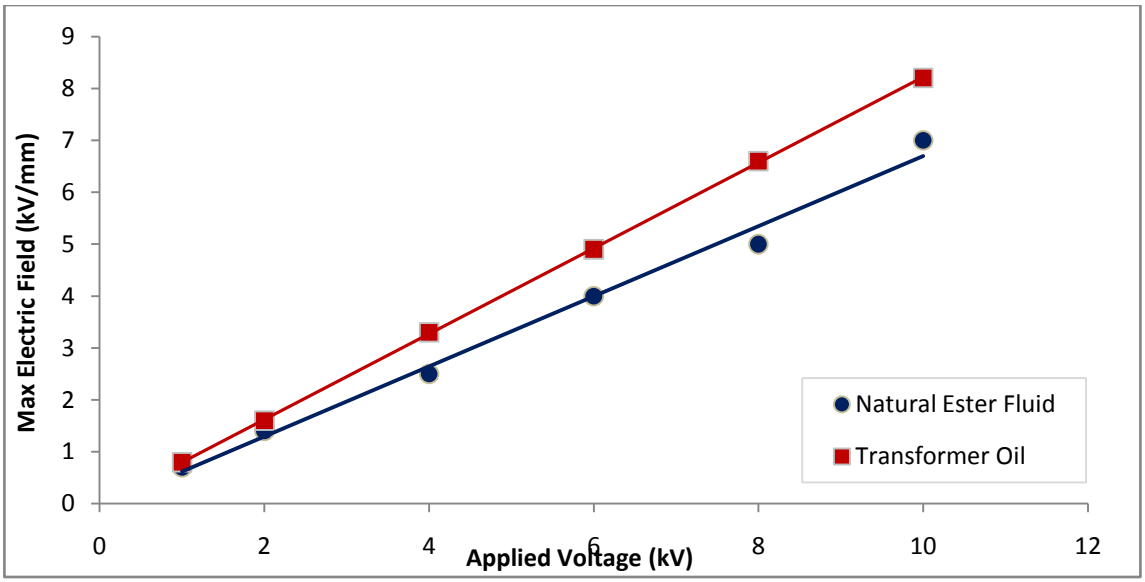

Figure 4.20: Relationship between applied voltage and maximum Electric field in elevated rod configuration

4.6.4 Influence of Microbubbles on the Field Distribution

4.6.4.1 Influence of micro bubbles of air

Point to plane geometry: Electric field distribution in the natural ester and transformer oil systems is shown in plate ix. The air bubbles slightly enhanced the maximum field in the system. The maximum field produced at the same applied voltage is almost equal but slightly greater in the transformer oil. An indication that presence of voids in natural ester is less disastrous compared with same amount of voids in mineral oil.

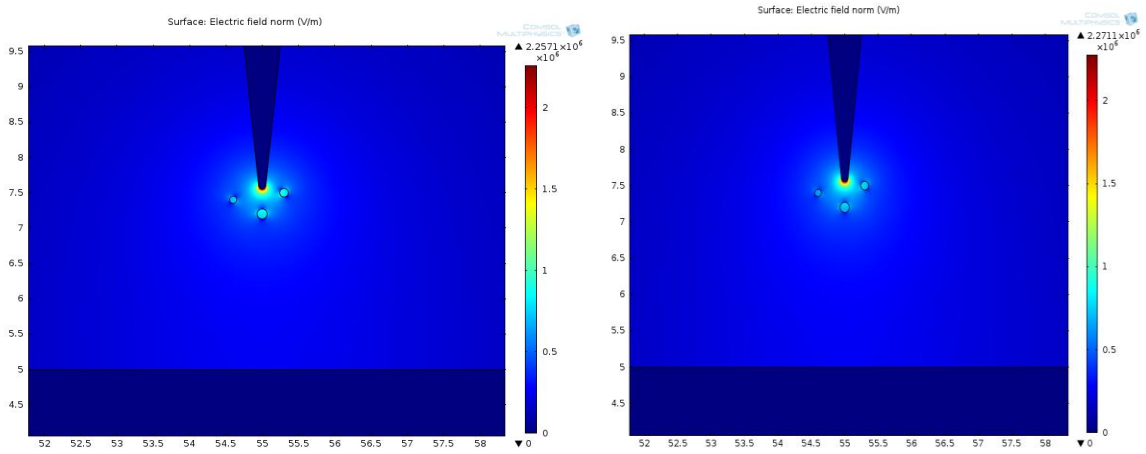

Plate IX: Electric field distribution in point to plane configuration with injected air bubbles at applied voltage of 1Kv (a) in Natural Ester Fluid, (b) in Transformer Oil

Rod to plane geometry: Similar to the point plane electrode geometry model, the maximum field produced is greater in the transformer oil than in the natural ester fluid**.**

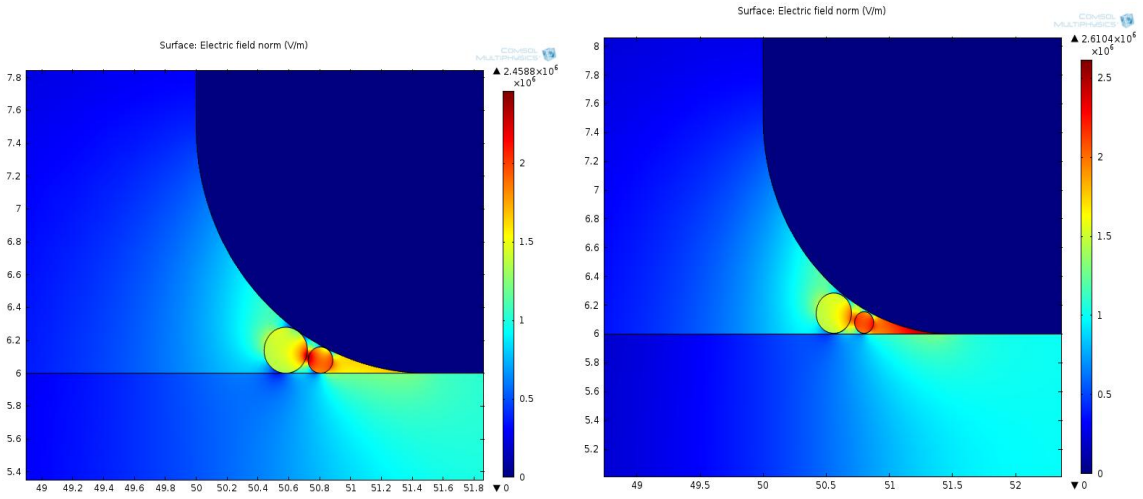

Plate X: Electric field distributions in presence of microbubbles of air at wedge region at an applied voltage of 1kV (a) in Natural Ester Fluid, and (b) in Transformer oil

Table 4.9: correlation between applied voltage and maximum electric field with injected air micro bubbles in the rod to plane configuration

S/No	Applied Voltage(kV)	Maximum Electric Field(kV/mm)	
		Natural Ester Fluid	Transformer Oil
1	1.0	2.00	2.60
2	2.0	4.50	5.20
3	4.0	9.00	10.0
4	6.0	14.0	16.0
5	8.0	18.0	21.0
6	10.0	20.0	26.0

The linear relation between the applied voltage and maximum electric field is plotted;

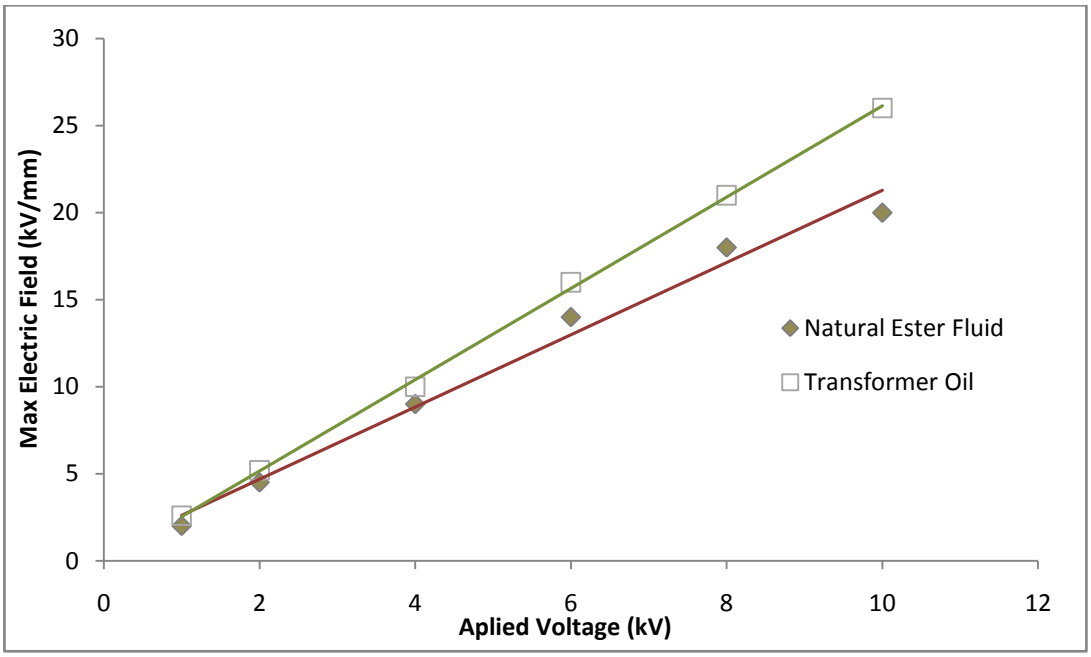

Figure 4.21: Relationship between applied voltage and maximum electric field in the rod plane configuration with injected air micro bubbles

Elevated rod geometry: In this configuration, voids has same effect on both mineral oil and natural ester fluid.

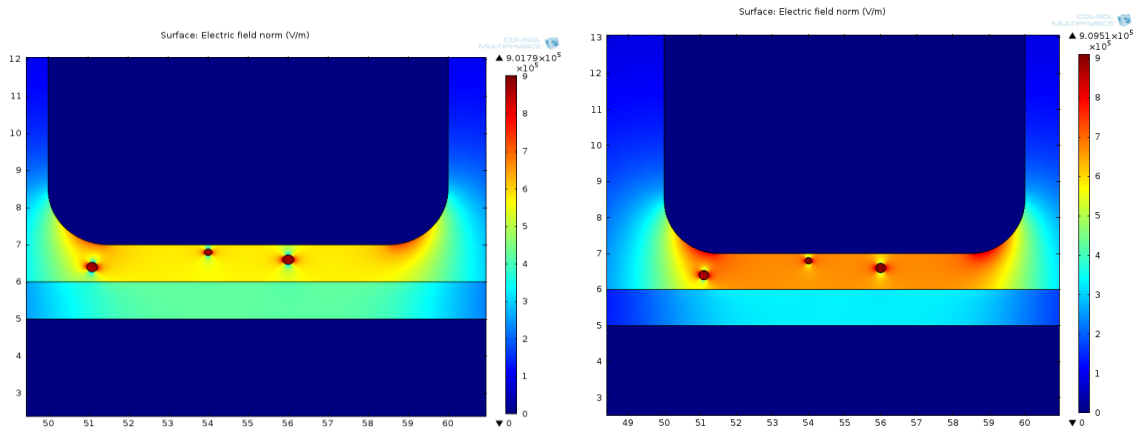

Plate xi: Electric field distribution in presence of air microbubbles at strong field region at an applied voltage of 1kV (a) in Natural Ester Fluid, and (b) in Transformer Oil

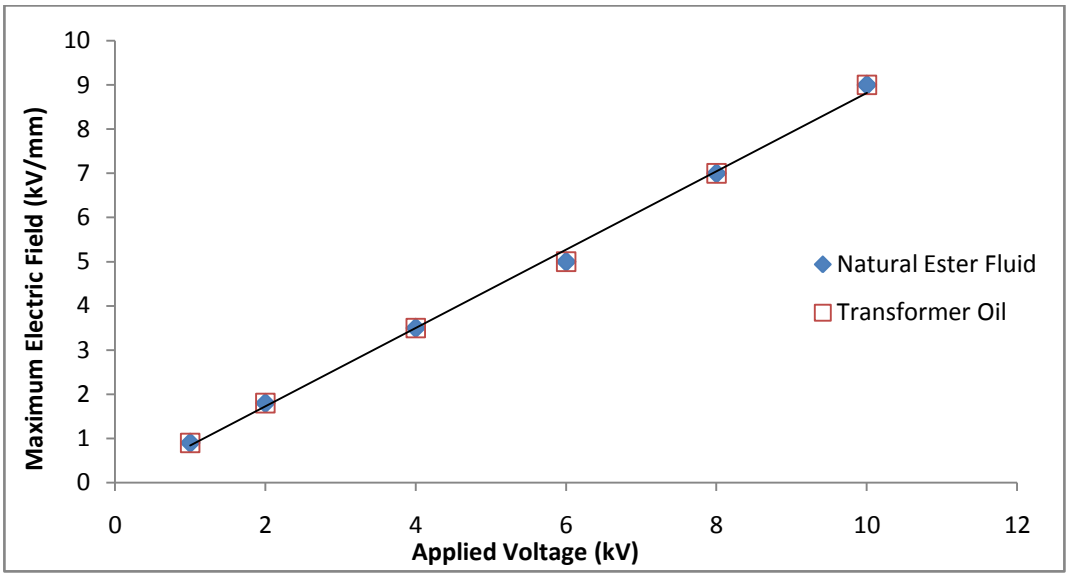

Figure 4.22: Relationship between applied voltage and maximum electric field in elevated rod configuration with injected air micro bubbles

4.6.4.2 Influence of water micro-bubbles

Point to plane configuration: The moisture enhanced the maximum field and the field enhancement is higher than that of air bubble. The maximum field produced at the same applied voltage is almost equal but slightly greater in the transformer oil. An indication that presence of moisture in natural ester is less disastrous compared with same amount of moisture in mineral oil.

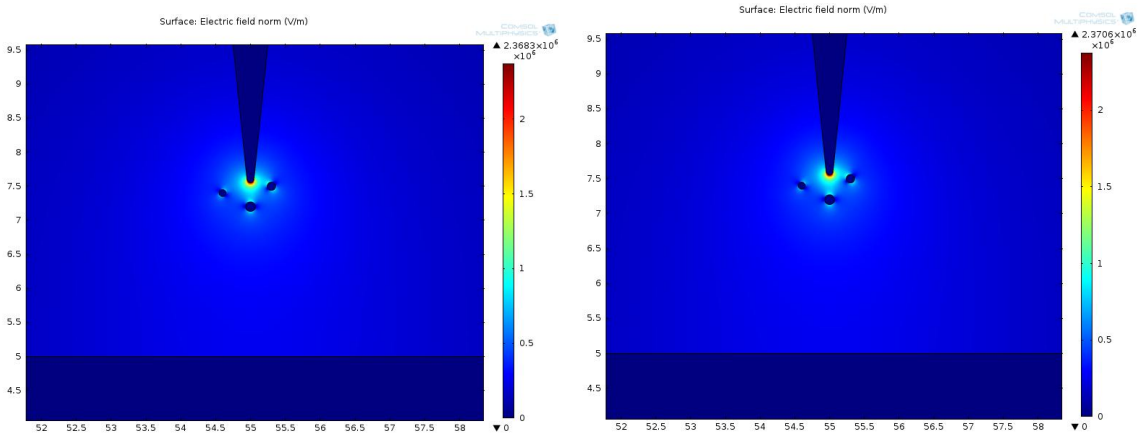

Plate xii: Electric field distribution in point to plane configuration with injected water bubbles at applied voltage of 1 kV (a) in Natural Ester Fluid (b) in Transformer Oil

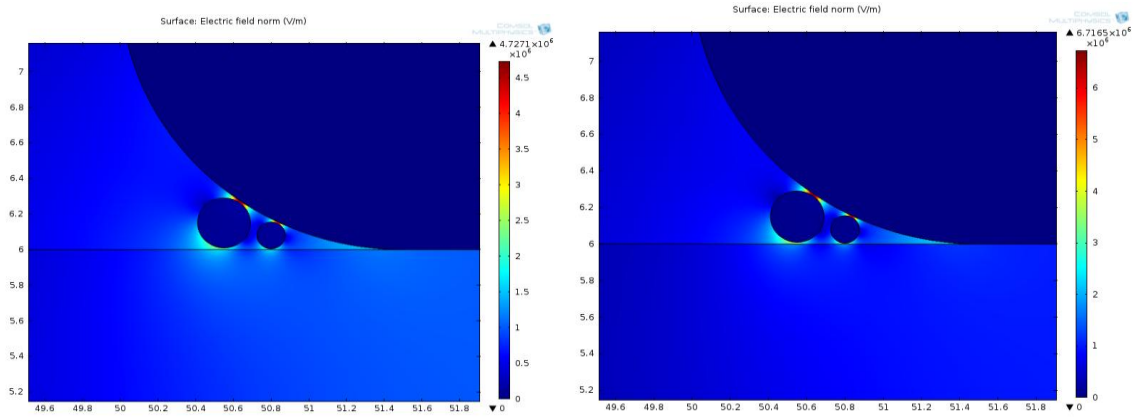

Plate xiii: Effect of water micro-bubbles on electric field distribution at applied voltage of 1 kV (a) in natural ester fluid, and (b) in Transformer Oil

Rod to plane configuration: Water bubbles was also simulated around the wedge of the rod to study its influence on the field distribution. The plots of the field distribution are shown in plate xiv. Maximum field of about 6.7 kV/mm is produced in transformer oil against 4.7 kV/mm produced in the natural ester fluid at the same applied voltage. This is an indication that the presence of moisture around the triple region has significant effect on the field distribution.

The field is higher in mineral oil (transformer oil) than in the Natural ester fluid. The linear relationship between the applied voltage and maximum electric field is plotted;

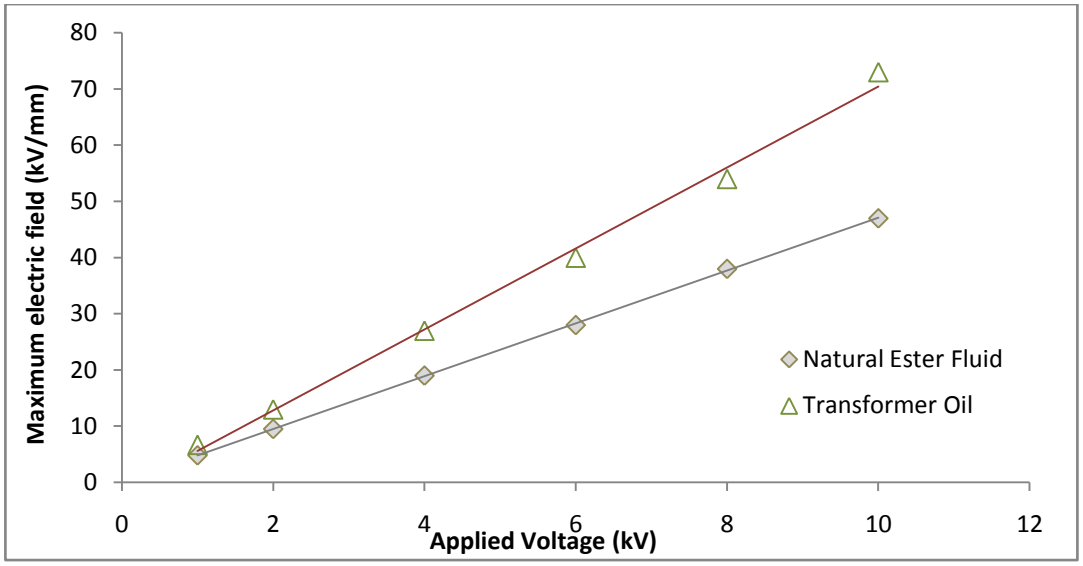

Figure 4.23: Relationship between applied voltage and maximum electric field in rod to plane configuration with injected water micro bubbles

Elevated rod geometry: Presence of water bubble in the insulating fluid between the voltage electrode and the solid insulation is simulated in plate xv. The field enhancement by the moisture impurity is higher in mineral oil when compared with natural ester fluid.

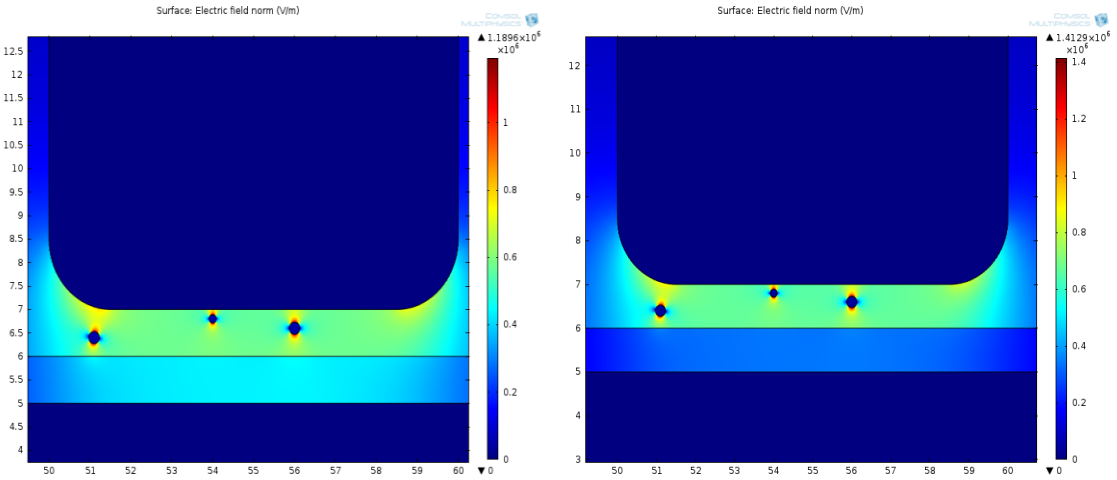

Plate xiv: Electric field distribution in presence of water microbubbles at strong field region at an applied voltage of 1 kV (a) in Natural Ester Fluid, and (b) in Transformer oil

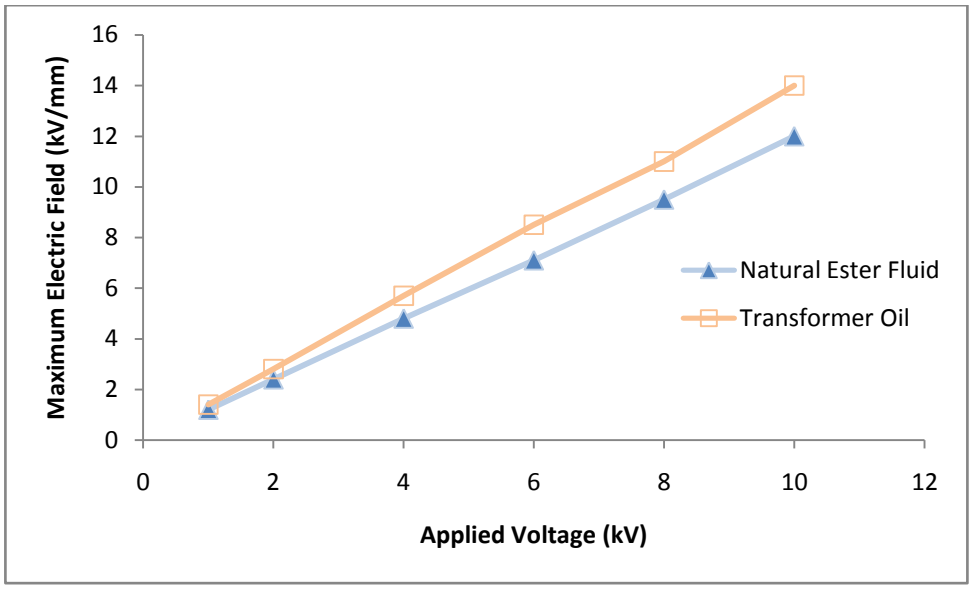

Figure 4.24: Relationship between applied voltage and maximum electric field in the elevated rod configuration with injected water bubbles

CHARPTER FIVE

DISCUSION

5.1 Discussion on Experimental Results

After purification, the PNO sample possesses absorption band about 1660 cm^{-1} which is typical of C=C stretching vibration as shown in figure 4.1. The absence of these bans in the two other samples (ENO and ENOE) is as a result of conversion of the double bonds in the PNO in an epoxidation reaction. The chemical modification effectively converted the unsaturation (carbon double bond) present in some of the fatty acids in the neem oil sample. The epoxy fingerprints appeared around peaks at 844 and 829cm^{-1} (Abdelmalik *et al.*, 2014), this confirms the conversion of unsaturation in the oil to epoxide. The chemical modification performed was effective in the elimination of unsaturation in the oil making it thermally stable to oxidation at elevated temperatures.

Viscosity is one of the many properties of the fluids studied. From the viscosity values presented in table 4.1, epoxidation was observed to alter viscosity of the oil. The viscosity increased with epoxidation. The observed increase in viscosity is as a result of the introduction of epoxy ring in the structure of the long chain fatty acids. This is agrees with the report on the epoxidation of another vegetable oil (Abdelmalik *et al.*, 2014). The presence of epoxy ring appears to have increased the resistive force between the layers of oil. On transesterification, the viscosity of ENOE was found to be lower than the viscosity of ENO at same temperature. This is the consequence of the high molecular weight glycerol that was removed from the epoxy oil. But the viscosity is still higher than the viscosity of PNO. This is an indication that the epoxy group dominate the factors that

control the viscosity of the fluid The developed epoxy ester product was found to possess a relatively high viscosity compared with the FR3 natural ester fluid. FR3 natural fluid is an insulating fluid with registered trade mark Enverotemp FR3 fluid of cooper power systems.It is synthesized from soya bean oil which has high percentage saturated fatty acid.

The viscosities of the samples show general pattern of variation with temperature (figure 4.6), viscosity is observed to decrease with increasein temperature as is common with most seed oils, and is consistent with the Arrhenius-type equation. Viscosity in liquids arises due to inter layer interactions (friction between layers), however, when heated, the interlayer interactions decreases hence decrease in viscosity of the samples with increasing temperature. Heat gain by the molecules of samples led to an increase in their kinetic energy, molecules of the liquid are freer to move about in the liquid, mobility increases and consequently leading to a decreasing inter layer force with increase in temperature as layers of the fluid can now easily slide over one another.

A two electrode coaxial cylindrical test cell was constructed for use in measuring the permittivity, loss tangent and conductivity of the samples. Measurement taken with the designed test cell was compared to standard measurements using some standard solvents. From figure 4.5, relative permittivity is observed to be frequency independent within frequency range of 20 Hz to about 100 kHz, this is an indication of a constant dominating conduction mechanism in the samples. However, the observed sharp rise of the dielectric constant at the vicinity of $50\ Hz$ (power frequency) could be as a result of resonance effect in the system or noise interference from some electrical appliances in the laboratory. The permittivity began to increase as frequency increases at higher frequencies $> 100\ kHz$ which is due to increase in dipole polarized particles in the fluids. The permittivity of the

sample is observed to slightly increase with processing. At fixed temperature and frequency, the samples have permittivities in the order ENO>ENOE>PNO. There seems to be a relationship between the viscosity of the fluids and permittivity. The ENO sample has the greatest viscosity, followed by the ENOE sample and then the PNO sample, the higher the viscosity the higher the permittivity value measured. The permittivity of a dielectric material determines its ability to store energy as a direct consequence of polarization in the material. The increased permittivity could be as a result of increased ionic impurities in the fluids during process of modification.

Due to the polar nature of seed oils, two factors contribute to losses in them; conduction processes and polarization phenomena. From the log-log plots in figures 4.6 of the loss tangent or dissipation factor against frequency at fixed temperatures, it is observed that loss tangent deceases with increasing frequency at low frequencies this is in agreement with equation 2.31; at low frequencies the effect of ionic conductivity is inversely proportional to frequency. Since ionic conductivity only introduces losses into the material as there is always certain inertia due to the movement of their masses, this implies that ionic conduction dominates in this frequency range and the graph maintain a -1 slope value in this range.

However, the sharp rise at vicinity of 50 Hz, is attributed to resonance effect in the circuit or noise interference from the ambience. Large amount of energy is dissipated consequently leading to the observed rise in loss tangent. At higher frequencies beyond 15 kHz, the loss tangent increases with increasing frequency and a transition from a negative slope value to a positive slope value is observed. This is because at high frequencies both dipole oscillation and ionic conduction contribute to losses in seed oils (Shah *et al.*, 2011).

The loss tangent in the samples increased with change in temperature which is as a result of increase in ionic conduction, electric conduction in the fluids contributes to loss in the material consistent with equation 2.37. Low loss materials are required in high voltage insulation. The loss is less than one (<1) in all the samples at the same frequency and temperature as shown in table 4.6. FR3 natural ester have loss tangent equal or less than 0.20 at 25°C (Dielectric fluid, 2010). Hence the developed fluid could serve as an alternative to the transformer oil.

Frequency dependence of the electrical conductivity at low frequency end of 20 Hz to 15 kHz is weak. The ac conductivity increased slightly with frequency raise in this range consistent with equation 2.36. Charges responsible for conduction in the liquid result from dissociation of ionic and solid impurities in the liquid and also from injection at the electrodes (Zadeh, 2011). At low frequency charges are able to migrate freely in the liquid hence leading to increase in conductivity with increasing frequency. Conductivity at high frequency is due to both ionic conduction and polarization effects. The increase in conductivity with increasing temperature in the samples represented in figure 4.14 is attributed to the change in viscosity with temperature. Decrease in viscosity with rise in temperature enhanced the mobility of charged particles in the liquids which resulted in more charge carriers contributing to electric conduction in the samples.

The linear variation of the ac conductivity with temperature in the Arrhenius plot (figure 4.15) is an indication of a thermally activated transport mechanism. Therefore, an increase in temperature resulted in more charge carries gaining kinetic energy and migrating leading to increase in conductivity in the samples. The increase in ac conductivity with increase in temperature is as a result of increase in dielectric loss due to polarization.

The viscosity and ac conductivity of the samples increased with processing. But particle mobility decreases with increase in viscosity in fluids as such increased ion concentration in the fluids could be responsible for the increase in conductivity. The increased concentration may have resulted from impurities formed or introduced during processing stages. Activation energy for electric conductivity indicates the difficulty experienced by charged particles in contributing to conduction in the viscous liquids. The PNO sample has activation energy of 0.41 eV which decreased with processing to values of 0.27 eV and 0.31 eV in ENO and ENOE samples respectively. The decreasing activation energy suggests that impurity give rise to conductions through low potential barrier.

5.2 Surface discharge development in oil-paper configuration

In the investigation of pre-breakdown events in transformer oil, the point to plane gap electrode configuration is the most favorable because even with the application of moderate voltages it produce high electric field and it reveals any polarity dependence of electric discharge. This is because small amount of charge on the tip can provide large surface density and a high density means a high field just outside the tip. However, in real power transformers the point to plane geometry is often present in the shape of a conducting particle either stuck at a barrier of freely moving in the bulk oil. As shown in plate iv, the electric field is concentrated around the tip of the high voltage point electrode and evolves into a low field towards the grounded electrode. Table 4.6 show the correlation between the applied voltage and the maximum electric field strength produced in the system for both the developed ester fluid and Mineral oil (Transformer Oil). The applied voltage has linear relation with the maximum electric field, the more the applied voltage the more the field intensity. According to Gauss law; the flux of electric field produced in a

region of the oil is proportional to the charge in the region. Hence maximum field regions are highly stressed regions and vulnerable to discharge. From the result, it is evident that the presence of conducting particles in the oil could lead to intense electrically stressed regions in the bulk of the oil which could lead local breakdown (partial discharges). Hence if the oil is to be used as insulating fluid in power transformers, it must be free of conducting particles. The maximum field intensity is also shown to be a function of the arc length (distance between the high voltage electrode and the ground electrode); becoming more intense with decrease in arc length.

Electric field distribution in any system depend on the electrode configuration, unlike the point to plane electrode in which moderate voltage when applied produces high electric field around the tip of the electrode, a voltage of 1 kV as applied produce maximum electric field of 1.6 kV/mm and 2.5 kV/mm in the natural ester and transformer oil concentrated around the triple junction of the high voltage electrode and the Kraft paper insulation interface, electrons are most likely to be emitted at this region (Chen *et al.*, 2012). Wedge shaped regions around conductors in oil-filled transformers are electrically stressed regions. This is because electric field around curved surfaces tends to be higher than near flat plane. The Kraft paper reduces the electric field in the oil which lead to increased field within the cellulose fiber (Kraft), although the breakdown voltage of cellulose is usually higher than that of seed oil, risk area for electric discharge remains in the wedge shaped regions around conductors. From the simulation result, it can be seen that the developed natural ester fluid has greater breakdown strength compared to the transformer oil.

As shown in plate vii, the high field region is concentrated around the wedge area of the high voltage electrode and in the oil space in between the high voltage electrode and the Kraft paper. Electrons are more likely to be emitted in this region of high electric field and consequently leading to breakdown. It is observed that in the rod to plane electrode, electric stressed region in the oil is reduced compare to the elevated case. The Kraft paper takes in most of the electric field from the oil. The use of paper electric insulation reduces risk of discharge in the oil in such configuration than in the elevated rod configuration.

The existence of air bubbles have significant influence on the development of surface discharges, air bubbles may originate from respiration of dielectric liquid, especially in open type power transformers, or from molecular evaporation in local high electric field strength regions or it could also originate from chemical bond breakage as a result of mechanical stress and thermal effect resulting from partial discharges. Due to the conservation of electric flux and the relatively lower permittivity of air, the electric field strength is higher than in the surrounding vegetable oil and Kraft paper. The maximum electric field region exists in within the inner surface of the bubbles, with magnitude of about 24 kV/mm as shown in plate viii. It is much more than the critical breakdown value for air which is 3 kV/mm. therefore, the high electric field in the bubble would lead to self-sustained discharge in the bubbles. Free electrons are released in the process and accelerated to impact the liquid molecule nearby (Chen *et al.*, 2012).

Water has high permittivity compared with the natural ester, high field region exist outside the water bubbles. For the same value of applied voltage it is observed from the correlation tables that the maximum field produced is higher when micro-bubbles are present. There is no doubt that the presence of air bubbles in the oil increases the risk of discharge in the oil.

CHARPTER SIX

SUMMARY AND CONCLUSION

6.1 Summary

Analysis of Nigerian neem oil as alternative dielectric fluid has been performed. The viscosity of the purified oil was found to be comparable with the commercially available ester insulating fluid. The viscosity was found have increased significantly after epoxidation. Transesterification was found not to have so much impact on the viscosity. Since the oil have inherent low melting point, and the chemical structural modification through epoxidation created thermo-oxidative stable neem oil and makes it suitable for industrial application that is open to air, moisture and elevated temperature.

The chemical processing was found to influence the electric conduction properties of the oil. The purified need oil has lower conductivity of the order of 10^{-9} S/m and this conductivity can still be reduced with better filtering system. Epoxidation and transesterification however lead to an increase in the conductivity by a factor of 2. This makes it interesting and suitable for a different industrial application. The low conductivity and loss makes it useful as insulating fluid while the increased conductivity makes it suitable as a potential based fluid for oil-base drilling fluid.

Simulation with of PNO fluid using different electrode configuration show that the developed fluid has superior breakdown properties comparable to existing natural ester transformer fluid. Natural ester fluid has high moisture absorption capability. The presence of moisture as impurities has less degradation impact as compare with mineral oil.

6.2 Contribution

- Purified neem oil, epoxy neem oil and epoxy neem ester have been developed from Nigerian available crude neem oil
- Chemical modification of neem oil produced interesting properties that makes neem oil useful as industrial fluid.
- The viscosity and low conductivity of purified neem oil makes a potential alternative insulating fluid.
- Epoxidation lead to increased viscosity and thermal stability. This makes it a potential stabilizing agent
- The higher conductivity and thermal stability of the epoxy neem ester makes a potential base fluid for drilling fluid.

6.3 Recommendation

In this research only a few of the many properties of insulating fluid were measured. Even though the obtained results shows that the use of PNO as insulating fluid is promising, determination of properties such as pour point, flash point, oxidative offset temperature, breakdown voltage etc will provide comprehensive information on the performance of the oil as insulating fluid.

Electric conductivity of the developed ester fluid is high compared with some existing natural ester fluid and mineral oil (transformer oil). Further purification of the ester fluid to reduce conductivity is necessary to avoid the possibility of dielectric heating.

And, an investigation of the electrical, thermal and rheological behaviour of aged sample of the developed fluid is recommended to ascertain it use over time in power systems.

6.4 Limitations

The research suffered limitations in area of electric failures; research took longer time then necessary and storage of samples was also difficult due temperature requirement for storing in a refrigerator.

And, due to the size of the test cell used, only small volume of the oil could be examined hence costing of the oil in other to make comparison to commercially available bio-base insulating fluid was difficult.

The frequency range consider was due to the constraint by the LCR Bridge with frequency range between 20 Hz and 200 kHz. Dispersion behaviour of the dielectric material in range of frequencies bellow 20 Hz and above 200 kHz could not be investigated.

REFERENCES

Abdelmalika, A.A., Abbottb, A.P., Fothergill, J.C.,Dodda, S. and Harris, R.C. (2010).Synthesis of a base-stock for electrical insulating fluid based on palm kernel oil.*Industrial Crops and Products*, 33: 532-536.

Abdelmalik, A.A, Fothergill, J.C., Dodd, S.J., Abbott, A.P. & Harris, R.C. (2011).Effect Of Side Chains On The Dielectric Properties Of Alkyl Esters Derived From Palm Kernel Oil. *Proceedings-IEEE International Conference on Dielectric Liquids*, ISSN 2153-3725.

Abdelmalik, A.A. (2014).Charge Dynamics in Vegetable Oil-Based Ester Dielectric Fluid.*British Journal of Applied Science and Technology*. 4(2): 371-386

Ahmad, Z. (2012).Polymeric Dielectric Materials. In: Silaghi, M.A., *Dielectric Material*, InTech, Croatia. pp. 4-6.

Atabani, A.E., Silitonga, A.S., Ong, H.C., Mahlia, T.M.I., Masjuki, H.H.,AnjumBadruddin,I. and Fayaz, H. (2013). Non-edible vegetable oils: A critical evaluation of oil extraction, fatty acid compositions, biodiesel production, characteristics, engine performance and emissions production. *Elsevier,*18: 211–245.

Berg, G. and Lundgaard, L.E. (1999) Discharges in Combined Transformer Oil/Paper Insulation.*Proceeding of 13th International Conference on Dielectric Liquids,* Nara, Japan. 20-25

Bartnikas, R. (2000) *Dielectrics and Insulators*.The Electrical Engineering Handbook. Boca Raton, CRC Press LLC. (55) pp. 1-20.

Callister, W.D. (2001). 5th ed, *Fundamental of Material Science and Engineering*.Wiley, New York.pp. S99-S109.

Chen, W., Chen, X., Su, X. and Long, Z. (2012). Simulation and analysis of surface discharge development in oil immersed paper insulation. *PrzegladElektrotechniczny, Electrical Review*. ISSN 0033-2097 R88NR9a. 290-295

Dielectric constants of solvents, Louisiana State University Macromolecular Studies Group Server, http/macro.lsu.edu/howto/solvents/Dielectric Constant.ht, Retrieved 7th September, 2014.

Dielectric Fluid (2010). *Cooper power systems*, Electrical Apparatus.900-20. Pp 1.

Duy, C.T., Lesaint, O., Bonifaci, N., Denat, A. and Bertrand, Y. (2007).High Voltage Breakdown and Pre-Breakdown Properties in Rape-seed Insulating Oil.Proceedings of the Annual Report *Conference on Electrical Insulation and Dielectric Phenomena*.1-7

Erhan, S.Z. and Asadauskas, S. (2000).Lubricant Base Stocks from Vegetable Oils.*Industrial Crops Products*, 11: 277-282.

Ethylene Structure, Retrieved February 14, 2015 from http/www.meritnation.com

Garces, R., Force, E.M. and Salas, J.J. (2011).Vegetable Oil Base-stocks for Lubricants.*GrasasAceites*, 62(1), *Enero-Marzo*, 21-28. ISSN: 0017-3495.

Gilson, M.K. (2006). Introduction to Continuum Electrostatics with Molecular Applications. Pp. 1-6.

Hwang, H.S. and Erhan, S.Z. (2001).Modification of Epoxidized Soybean Oil for Lubricant Formulation with Improved Oxidative Stability and Low Pour point. JAOCS, Vol 78: 1179-1184.

Hwang, G., Jadidian, J. and Zahn, M. (2009-2010). Mechanisms Behind Positive Streamers and Their Distinct Propagation Modes in Transformer Oil. In:*Progress report 152*, Zaahn, M., High-Voltage Dielectric Materials.*Research Laboratory Electronics (RLE).*pp. 1-3.

Jain, A.K. and Suhane, A. (2012).Research Approach and Prospects of Non-edble Vegetable Oil as a Potential Resource for Bio-lubricant-A Review.*Advanced Engineering and Applied Science.; an international Journal*. 1(1): 23-32.

Kaplan and McReynolds, B. (2002).Dielectric Characteristics of Materials-Electrostatic Discharge.In: Selvaduray, G., *MMatE210, Experimental Methods in Material Engineering*, Fall 2002. pp 1-22.

Kasap, S.O., Ruda, U. and Boucher, Y. (2002) 2nded, *Illustration Dictionary of Important Terms and Effects in Optoelectronics and Photonics.* pp.25.

Knothe, G. (2007) Epoxidation, hydroxylation and oxidative fission. In: Gunstone, F.D., Harwood, J.L., and Dijkstra, A.J., *The Lipid Handbook*. 3rd ed., CRC Press, Boca Raton.pp 546-548

Lucas, J.R., Abeysundara, D.C., Weerakoon, C., Perera, K.B.M., Obadage, K.C. and Gunatunga, K.I.A. (2001). Coconut Oil Insulated Distribution Transformer. 8th Annual *Conference of IEE Sri Lanka*. 1-5

Martinsen, W. (2011).A coaxial test cell for measuring electrical parameters of a sample of the ground surrounding a HF Antenna installation.*Defence Science and Technology Organization Publication*, Australia. 1-71

McMurry, J. (2011). 7thed, *Fundamentals of Organic Chemistry*.Brooks/Cole, USA.pp. 539-542

Marrtin, D., Wang, Z.D., Dyer, P., Darwin, A.W. and James, I.R. (2007). A Comparative Study of The Dielectric Strength of Ester Impregnated Cellulose for Use in Large Power Transformers. *2007 International Conference on Solid Dielectrics*. Winchester, UK. 8-13

Murphy, E.J. and Morgan, S.O. (2012).The Dielectric Properties of Insulating Materials.*Bell System Technological Journal.* 493-512

Oommen, T.V. (2002). Vegetable Oil for Liquid-Filled Transformers.*IEEE Electrical Insulation Magazine*, 18: 6-11.

Raju, G.G. (2003). *Dielectrics in Electric Field*. Marcel Dekker, Inc. New York. pp. 1-90.

Salimon,J., Salihu, N. and Yousif, E. (2011).Synthesis and Characterization of Physcochemical Properties of Oleic Acid Ether Derivatives as BiolubricantBasestocks.*Journal Oleo Science*, 60: 613-618.

Saremi, K. Tabarsa, T., Shakeri, A. and Babanalbandi A. (2012).Epoxidation of Soybean Oil.*Aannals of Biological Research*, 3 (9): 4254-4258.

Saroj, A.L. and Singh, R.K., (2011). Thermal, dielectric and conductivity studies on PVA/Ionic liquid [EMIM][EtSO4] based polymer electrolytes. *Elsevier; Journal of Physics and Chemistry of Solids.*73: 162-168

Saurabh, T., Patnai, M.K., Bhagt, S.L. and Renge, V.C. (2011).Epoxidation of Vegetable oils; A review.*International Journal of Advanced Engineering Technology*, 491-501.

Scrimgeour (2005).6thed, *Chemistry of Fatty Acids*. Willey, New York.pp. 1-44.

Shah, Z.H. and Tahir, Q.A. (2011).Dielectric properties of vegetable oil. Journal of Scientific Research, 3(3), 481-492.

Sharipov, R.V. (2003).*Classical Electrodynamics and Theory of Relativity*. Pp. 15-17.

Silverstein, R.M., Webster, F.X., and Kiemle, D.J. (2005). 7thed, *Spectroscopic Identification of Organic Compounds.* John Wiley and Sons Inc., USA. Pp 72-73

Standared Test Method for Dissipation Factor and Relative Permittivity of Electrical Insulating Liquids (1999) Annual Book of ASTM Standards, volume 10.03: Electrical Insulating Liquids and Gases; Electrical Protective Equipment.Pp. 54-58.

Stuart, B. (2004). *Infrared Spectroscopy: Fundamentals and Applications*. Wiley.Pp 1-28

Top-Notch Technology in Production of Oils and Fats. Retrieved September 10, 2014, from http/www.chempro.in

Willing, A. (2001).Lubricant Based on Renewable Sources-An Environmentally Compatible Alternative to Mineral Oil Products.*Chemosphere*, 43: 89-98.

William, D.B., Hess, H., Desai, V. and Deen, M.J. (2006).*Dielectrics*. The Electrochemical Society Interface, Spring. (15) 1

Zadeh, M.S. (2011). Measurment of ion mobility in dielectric liquids.*Chalmers Reproservice,* Sweeden. pp. 1-71.

Zahn, M. (2003).*Electromagnetic Field Theory*: A problem solving approach, Robert E.Krieger publishing compay Inc. pp. 135-143

Appendix I

Drawing of the coaxial test cell

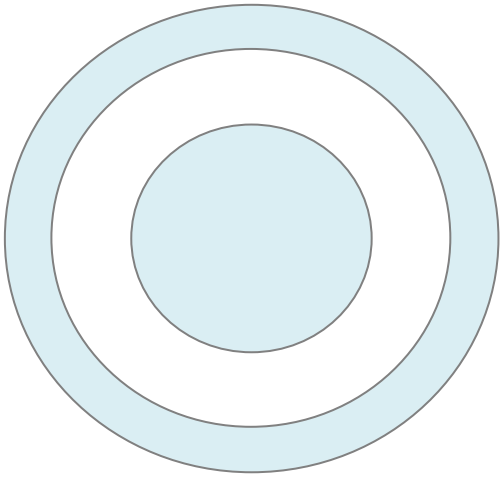

Top view of the two concentric electrodes

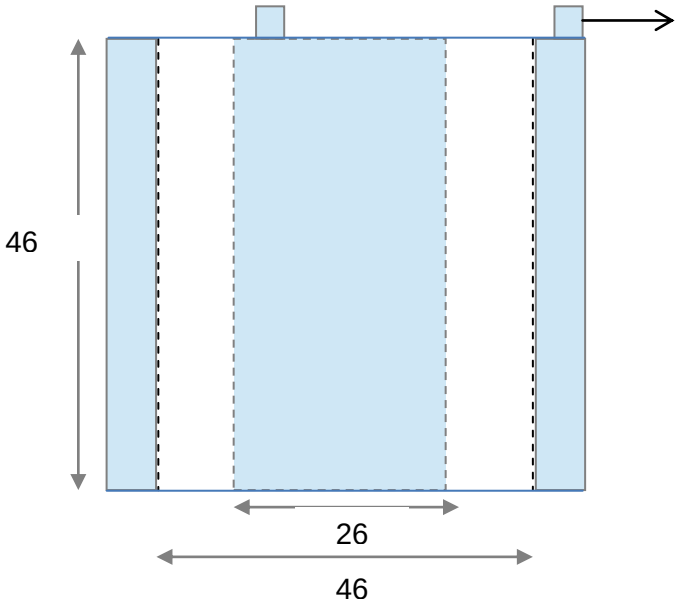

Side view of the coaxial electrodes

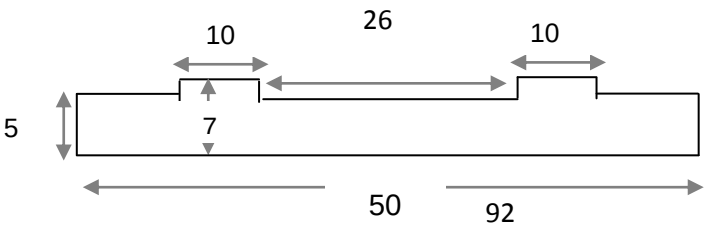

Side view of the insulating base

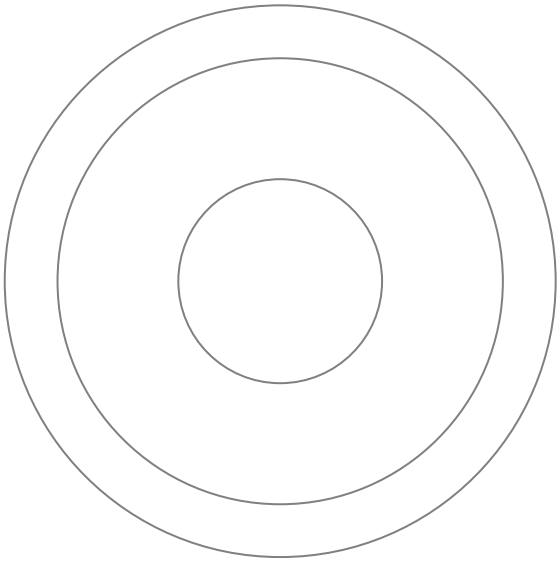

Top view of the Base

Side view (The dash lines shows inside line that are not visible from the outer cylinder)

Appendix II Error calculation in measurement using the LCR Bridge

Table ii: Accuracy table of the HM8118 LCR Bridge

Primary Parameter: Basic accuracy (Test voltage: 1.0V, measurement SLOW/MEDIUM, autoranging mode, constant voltage OFF, bias off). For FAST mode double the basic accuracy values

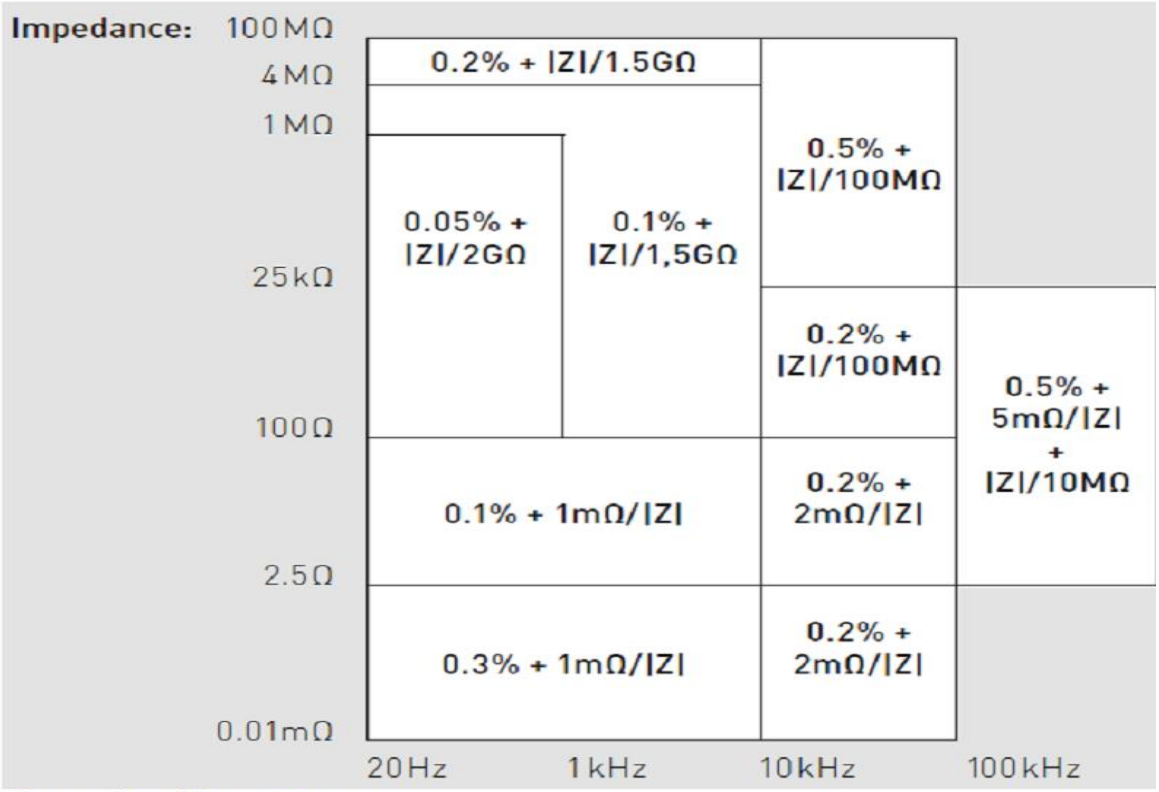

Secondary Parameter:

Basic accuracy D, Q: ±0.0001 @ f = 1 kHz

Phase angle: ±0.005° @ f = 1 kHz

Error in measurements using the LCR Bridge is calculated from the measured impedance value at a particular frequency. For an impedance of 687kΩ at a frequency of 1 kHz the error is calculated as follows;

$$Error = 0.5\% + \frac{|Z|}{100M\Omega} = 0.5\% + \frac{687\times10^{3}\Omega}{100\times10^{6}\Omega}$$ = 0.5% + 0.00687 = 0.5% + (0.00687*100%)

= 0.5% + 0.69% = 1.19%

Therefore, 1.19% is the percentage error in measuring the say capacitance at frequency of 1kHz.